Melting behaviour of the freeze plug in a molten salt fast reactor

by

I. Koks

in partial fulfilment of the requirements for the degree of

Bachelor of Science
in Applied Physics

at the Delft University of Technology.

Student number:	4299981
Date:	13-07-2016
Supervisor:	Dr M. Rohde
Committee:	Dr M. Rohde
	Prof. J.L. Kloosterman

Section of Nuclear Energy and Radiation Applications
Department of Radiation Science and Technology
Faculty of Applied Sciences

TU Delft Delft University of Technology

Abstract

The molten salt fast reactor (MSFR) is a generation IV reactor that is more sustainable and produces a minimum of waste. The safety of this reactor is guaranteed by a freeze plug that prevents the molten salt from flowing to the drainage tanks. In case of a station black-out or an overheating reactor, the freeze plug has to melt in order to drain the molten salt to the drainage tanks such that the reactor will not be damaged.
This thesis studies the melting behaviour of a new design of the freeze plug holder. In this new design the freeze plug will melt from the sides by convective heat transfer instead of only from the top.
First, the top of the freeze plug has to melt, such that the molten salt in the reactor vessel can flow past the plug. This will take 115 s. Once the molten salt flows past the freeze plug, the 'frozen' salt will melt from the sides. After 50 s, the freeze plug will drop down due to the large pressure on top of the plug and the liquid layer between the supporting metal ring around the freeze plug and the solid salt cylinder. When the freeze plug has dropped down, the remaining molten salt in the reactor has to flow to the drainage tanks, which will take at the utmost 80 s, as a part of the molten salt volume has already flown to the drainage tanks before the freeze plug has dropped down.
The total emergency drainage time in case of a station black-out is 245 s, which is below the maximum permitted time of 480 s, meaning it can be concluded that this new design of the freeze plug might work.

Acknowledgements

I would like to thank my supervisor Martin Rohde for his help during our meetings, I really learnt a lot from this project. I would also like to thank Parth Swaroop for his help with analysing and understanding the melting behaviour of the freeze plug. Furthermore I would like to thank Oliver van den Bergh and Chris van Egmond for their daily support and good conversations. It was really nice to work with you. And finally, I would like to thank Yvonne Koks for her help with the English language while writing my thesis.

Contents

List of Figures ix

List of Tables xi

Nomenclature xiii

1 Introduction 1
1.1 Generation IV reactors . . . 1
1.2 Fukushima accident. . . . 3
1.3 Requirements of the freeze plug . . . 3
1.4 Thesis outline . . . 4

2 Theory 7
2.1 Heat transfer . . . 7
2.1.1 Heat transfer with melting behaviour . . . 7
2.1.2 Conductive heat transfer . . . 9
2.1.3 Convective heat transfer . . . 9
2.1.4 Turbulence model. . . . 10
2.2 Drainage of the reactor. . . . 12

3 Modelling in COMSOL 13
3.1 Model 1: Melting behaviour one-dimensional rod. . . . 13
3.1.1 Newton-Raphson method . . . 14
3.2 Implementation of the molten salt . . . 15
3.3 Model 2: Convective heat transfer model . . . 15
3.3.1 Turbulence model. . . . 16
3.3.2 Wall functions. . . . 17
3.3.3 Influence Nusselt numbers on heat transfer . . . 17
3.4 Model 3: Radial melting behaviour freeze plug . . . 19
3.5 Model 4: Determination K-factor with turbulence model . . . 20

4 Results and Discussion 21
4.1 Model 1: Melting behaviour one-dimensional rod. . . . 21
4.2 Model 2: Convective heat transfer . . . 24
4.2.1 Turbulent flow . . . 24
4.2.2 Influence Nusselt numbers on heat transfer . . . 25
4.3 Model 3: Radial melting behaviour freeze plug . . . 26
4.4 Model 4: Determination of the K-factor. . . . 28
4.5 Model 5: Time to drain reactor vessel when a part of the freeze plug has melted from the top . . . 28
4.6 Emergency drainage time . . . 30
4.6.1 Determination $t_{melt,top}$ . . . 30
4.6.2 Determination t_{drop} . . . 30
4.6.3 Determination $t_{drain,rest}$ . . . 31
4.6.4 Total emergency drainage time . . . 31

5 Conclusion 33
5.1 Recommendations . . . 33
5.1.1 Other designs for the safety plug . . . 34

Bibliography 37

A Analytical solution 1D melting problem 39

B K-factor and drainage time 41

List of Figures

1.1 Different generations of nuclear reactors. [1] 1
1.2 Design of the Molten Salt Fast Reactor [2]. 2
1.3 The vertical cross sections of two designs of the freeze plug. In the old situation, the pipe contains one frozen piece of salt, which has to melt all the way from top to bottom. As this takes too long [3], a new design is proposed, as shown on the right side. 4

2.1 Freeze plug in its new holder design with the three heat transfer mechanisms shown. 7
2.2 A long, solid rod to which a temperature T_1, higher than the melting temperature T_m, is applied on one side. $T_{2,\infty}$ is lower than T_m. This drawing shows a two-dimensional situation of the melting problem, but the calculation of the melting front is only done for the one-dimensional situation, which means that there is no temperature gradient in the vertical direction in this figure. 8
2.3 Cylinder in axial flow as described in [4] 10

3.1 Newton method with starting point u_0. 15
3.2 Damped Newton method with starting point u_0 and damping factors α_0, α_1 and α_2. 15
3.3 Two-dimensional axisymmetric model of the freeze plug with a pipe added before and after the plug part. In the model, the pipe before and after the freeze plug is made extra long in order to let the velocity profile recover from the freeze plug. 16
3.4 Zoom of freeze plug in figure 3.3, where 5 cm has melted from the top, so that the fluid can only flow between the solid plug and the wall. 16
3.5 Free triangular finer mesh put on the geometry of which a zoom is made to the parts where the most complex turbulent flow occurs. 17
3.6 The velocity profile in a pipe (left) with a zoom on the wall region (right) [5]. Near the wall there are three layers: the viscous sublayer, the buffer layer and the log-law region. Each layer is described by another formula which cause different gradients to occur. 17
3.7 Two-dimensional axisymmetric model of the freeze plug and its holder in which the boundaries are indicated by a number. The right domain (rectangle) consists of hastelloy N and the left domain (square) consists of ice. 18
3.8 Zoom of the mapped mesh in the two-dimensional axisymmetric geometry shown in 3.7. 18
3.9 two-dimensional axisymmetric model of the freeze plug. The blue line represents the one-dimensional model as shown in figure 3.10. The red part is made of hastelloy N. 19
3.10 One-dimensional axisymmetric model of the freeze plug 19
3.11 Two-dimensional axisymmetric model of the freeze plug, in which lines 1 and 2 are drawn. On these lines the average pressure and velocity are calculated. . . 20

4.1 Temperature distribution at $t = 300$ s. The kink in the graph indicates the melting front. 21
4.2 Melted length of the ice versus time for different melting ranges applied in COMSOL. The larger the melting range, the closer it approaches the analytical solution. 22
4.3 Melted length to time for different mesh settings. 'Mesh 5000' means that there are 5000 elements in the rod and the number of seconds in the legend represents the time step taken in the time-dependent solver. 22

4.4 Figure 4.3 zoomed in for a better image of the differences between the solver settings. The finer the element size (the more elements in the mesh) and the smaller the time step taken in the solver, the more the modelled solution approaches the analytical one. 23
4.5 Comparison of melting behaviour of a one-dimensional rod between molten-solid salt system and water-ice system. 23
4.6 Turbulent flow in a two-dimensional axisymmetric model of the freeze plug. The direction of the arrows indicates the direction of the flow. The red circles indicate the recirculation areas. 24
4.7 Turbulent flow in a two-dimensional axisymmetric model of the freeze plug. The velocity magnitudes of the turbulent flow for an inlet velocity of $6.5\,\mathrm{m\,s^{-1}}$ are indicated. 25
4.8 Isothermal contours in freeze plug for t=300 s. Different heat fluxes have been applied on the top, axial and bottom boundaries. The melting front with $T = 273.15$ K is indicated extra clearly by the arrow. 26
4.9 Melting behaviour of one-dimensional radial freeze plug with hastelloy N wall and forced convection for the water-ice system. In this figure the melted length has been plotted for different settings of the element size in the mesh and the time step taken by the solver. 26
4.10 Comparison of the melting behaviour of a one-dimensional radial plug with and without the hastelloy N wall and forced convection for a mesh of 7000 elements and a time step taken of 0.5 s for the water-ice system. 27
4.11 Comparison of the melting behaviour of the molten-solid salt system and the water-ice system for a model of a one-dimension radial plug with a hastelloy N wall and forced convection for a mesh of 8000 elements and a time step of 0.1 s. 27
4.12 Determination of the K-factor, by applying a polynomial function to the solution generated by the model in COMSOL. 28
4.13 Schematic representation of the reactor system. Note that the reactor vessel has the modelled dimensions and not the actual ones. The image is not to scale. 29
4.14 The course of the height of the liquid in the modelled reactor vessel, starting with a full vessel of height 2.84 m. 29
4.15 Adjusted design for the freeze plug in order to reduce the linear melting time from the top. The blue part is removed to make the distance between the straight pipe (the top of the solid part in the beginning) and the top of the solid part once it has melted smaller. The necessary length to melt from the top is reduced from 5 cm to 1 cm. 30

5.1 Two new conceptual designs of the safety plug: the break plug and the mechanical plug. 35

List of Tables

1.1 Overview of the models in this thesis. 5

2.1 Parameters C and e in formula 2.12 for the Nusselt number of the heat transfer of a cylinder in an axial turbulent flow for different sides of the cylinder. 10
2.2 Constants in k-ϵ model. 12

3.1 Properties of solid and liquid water [6]. 14
3.2 Properties of molten salt LiF-ThF_4, where in all formulae temperature T is in K. The value of C_p for 700 °C is extrapolated, as it is out of the validity range. . . . 15

4.1 Properties of the two melting systems. 23

Nomenclature

Symbol	Description	Units
α_l	thermal diffusivity of liquid	$m^2\,s^{-1}$
α_s	thermal diffusivity of solid	$m^2\,s^{-1}$
δ	melted length	m
ϵ	rate of dissipation	$m^2\,s^{-3}$
ϵ_M	eddy diffusivity for momentum	$m^2\,s^{-1}$
λ_l	thermal conductivity of liquid	$W\,m^{-1}\,K^{-1}$
λ_s	thermal conductivity of solid	$W\,m^{-1}\,K^{-1}$
μ	dynamic viscosity	Pa s
ν	kinematic viscosity	$m^2\,s^{-1}$
ρ_s	density of solid	$kg\,m^{-3}$
C_p	specific heat	$J\,kg^{-1}\,K^{-1}$
D	characteristic length or hydraulic diameter	m
E	energy	J
e	turbulent kinetic energy	$J\,kg^{-1}$
f	Fanning friction factor	-
g	gravitation constant on earth, 9.81	$m\,s^{-2}$
H	height of the reactor vessel	m
h	convective heat transfer coefficient	$W\,m^{-2}\,K^{-1}$
h_{tank}	height of liquid level in reactor vessel	m
k	kinetic energy per unit volume	$J\,m^{-3}$
L	pipe length of drainage system	m
L_{fus}	latent heat of fusion	$J\,kg^{-1}$
Nu	dimensionless Nusselt number, ratio between total heat transfer and convective heat transfer	-
p	pressure	Pa
R_{pipe}	radius of the drainage pipe	m
R_{tank}	radius of the reactor vessel	m
Re	dimensionless Reynolds number, ratio between inertia forces and viscous forces	-
T	temperature	K

t	time	s
T_l	temperature of liquid	K
T_m	melting temperature	K
T_s	temperature of solid	K
T_w	temperature at the wall	K
v	velocity	$\mathrm{m\,s^{-1}}$
x	location in cartesian coordinates	m
z	height	m

1

Introduction

Since the nuclear accidents in Chernobyl (1986) and Fukushima (2011), faith in nuclear reactors has decreased. Apart from the risk of accidents, the current nuclear power plants produce nuclear waste that can last 10,000 years (with recycling in Europe), which makes it almost impossible to communicate the location of the storage facilities to future generations.

1.1. Generation IV reactors

This is why a new generation of nuclear reactors is being developed since 2000, called generation IV. These reactors are not only supposed to be more sustainable and economical, but also to produce a minimum of waste. The development of nuclear reactors over generations is shown in figure 1.1.

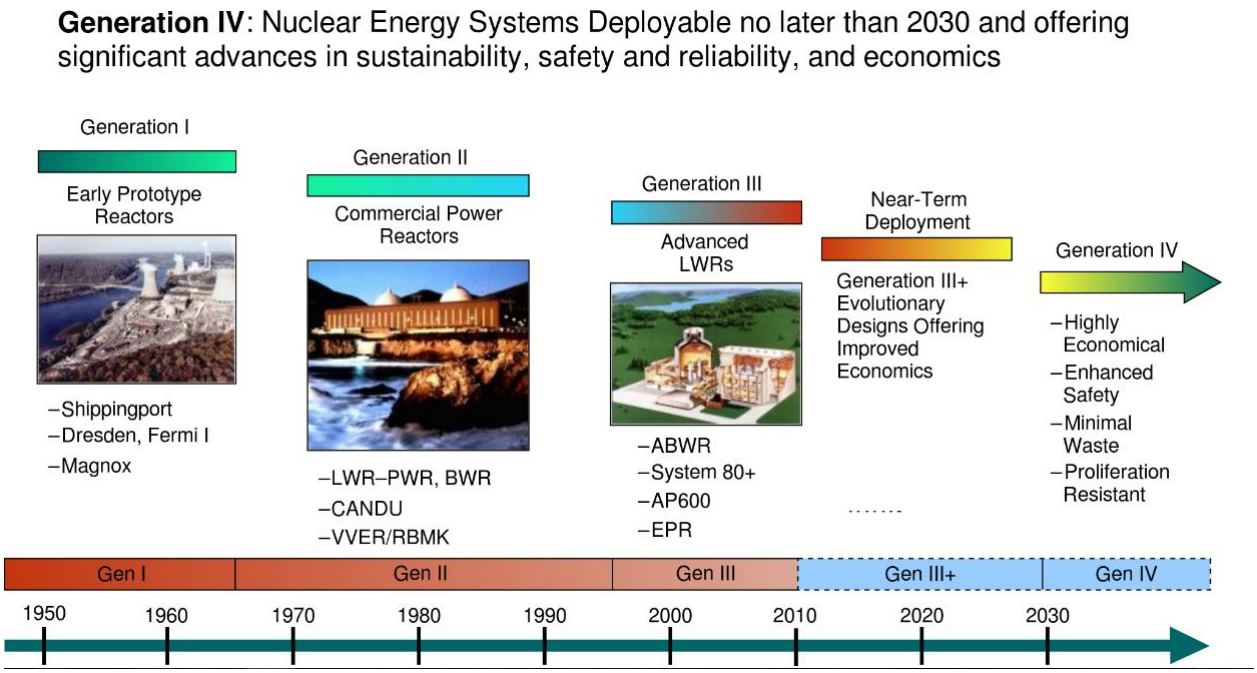

Figure 1.1: Different generations of nuclear reactors. [1]

Six new reactor types are scheduled for licensing between 2020 and 2040 [1]:

- Gas-Cooled Fast Reactor
- Lead-Cooled Fast Reactor
- Molten Salt Reactor
- Sodium-Cooled Fast Reactor
- Supercritical-Water-Cooled Reactor
- Very High Temperature Reactor

Among these, the Molten Salt Reactor seems the most promising, as it can burn minor actinides that currently remain in the waste of the current nuclear reactors.
As described in 'Overview and Perspectives of the MSR in generation IV' [2], the fuel in this reactor is dissolved in a molten salt, while the same liquid salt functions as a coolant. This idea started with the U.S. Aircraft Experiment in support of the U.S. Aircraft Nuclear Propulsion Program in the 1950s. The first used molten salt consisted of NaF-ZrF_4-UF_4 ($53-41-6$ mol%). During the 1960s, the Oak Ridge National Laboratory was the leader in the field of research regarding power reactor designs.

Currently, different types of molten salt reactors are being developed and examined, among which there is the Molten Salt Fast Reactor (MSFR). This type of reactor, the design of which is shown in 1.2, is the focus of this thesis.

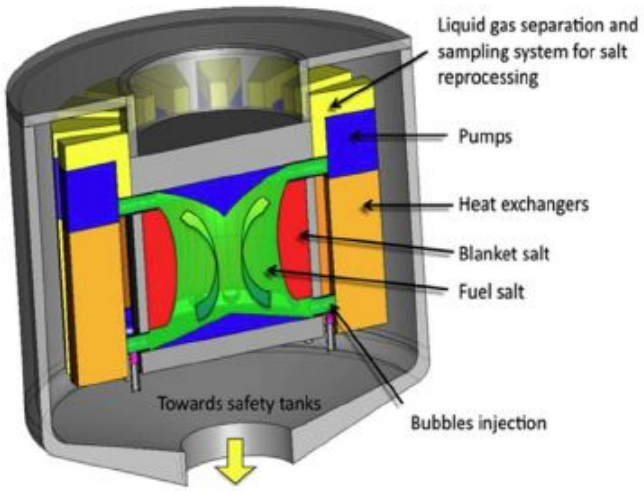

Figure 1.2: Design of the Molten Salt Fast Reactor [2].

In the MSFR, there is a fuel and a blanket salt, with the fuel salt carrying the fissile ^{233}U and the blanket salt carrying the fertile element thorium. When thorium captures the neutrons that come from fission of ^{233}U in the fuel salt, ^{233}U is produced in the blanket, which can then be reinjected in the fuel salt by fluorination. This chemical process converts UF_4 into UF_6 by bubbling fluorine gas through the salt. This UF_6 (gas) is then converted back to UF_4 before it is inserted into the fuel salt. In this way, there is a circulation of fissile elements in such a way that the initial fuel burns up.
The fuel salt consists of lithium fluoride, thorium fluoride and a heavy nucleus like uranium [2]. In the core, the fuel salt flows freely without any moderator, completing a full cycle in 3 to 4 seconds. The liquid fluoride fuel salt also functions as a coolant. As shown by figure 1.2, on its way back to the core, the fuel salt flows past heat exchangers, allowing the salt to give off part of its heat, which can then be used for generating electricity with a turbine. At

the end of the path of the molten salt, bubbles are injected for cleaning of the fuel salt.
The core's dimensions in the preliminary design are 2.25 m high by 2.25 m in diameter, with a total volume of the fuel salt is 18 m^3, of which approximately half is located in the core and the other half in the pipings and heat exchangers that form the external fuel circuit. [2]
The safety of the MSFR is guaranteed by the use of draining tanks and a freeze plug, located beneath the reactor core. The freeze plug keeps the molten salt in the reactor core and has to melt in two cases, which are explained in section 1.3. This thesis researches the design and melting behaviour of the freeze plug, whose requirements were tightened after the accident in Fukushima. The next section briefly describes the Fukushima disaster, to prove the necessity of tightening these requirements.

1.2. Fukushima accident

On 11 March 2011, an earthquake with a magnitude of 9.0 on the Richter magnitude scale, occurred in Japan. The epicentre of this 'Great East Japan Earthquake' was located in sea, so this already devastating earthquake was followed by a large tsunami with waves up to 30 m. The Fukushima Daiichi Nuclear Power Plant is located in the area affected by both the earthquake and the tsunami. During the earthquake, the three operating boiling water reactors were shut down, since the safety sensors detected the motion of the ground. When shut down, the reactors still needed to be cooled, because they continue to produce decay heat. Due to the earthquake there was a complete loss of off-site electricity, so on-site emergency diesel generators were used to deal with the decay heat.

Around 50 minutes later, the tsunami wave hit the shore, causing the NPP site to be inundated and several buildings to be damaged, including the building where the emergency diesel generators were located, resulting in a total loss of AC power on-site. Despite the design of the Fukushima Daiichi NPP, meant to withstand an electricity loss of 8 hours with DC batteries in each reactor, the flooding had also damaged this equipment and consequently, reactor units 1, 2 and 4 lacked cooling. Eventually unit 1 exploded, following by an explosion in unit 3. Cooling with sea water could not prevent this from happening. [7]

Nowadays, this Fukushima catastrophe serves as a learning point, clearly indicating the need for new design requirements. No safety equipment should be allowed to depend on electricity anymore, because in the unlikely event of all electricity supplies being damaged, which was the case in Fukushima, the reactor cannot be cooled anymore. For this reason the freeze plug should not be melted by an electrical heater. Instead, it needs to be able to melt under its own power, for example by using the liquid molten salt.

1.3. Requirements of the freeze plug

In normal operation, the freeze plug has to close the pipe to the drainage tanks. However, in two cases it has to melt in order to drain the reactor vessel:

- Station black-out
- Overheating reactor

A station black-out means there is an on-site power breakdown, because of a natural disaster or a political, technical or economical reason. Without electricity, all pumps and heating or cooling elements will stop working, which also means that the fuel salt in the core will start to heat up. If this process is allowed to continue, temperatures may reach critical levels resulting in reactor elements breaking down or melting.

The second case is when the reactor overheats. This can happen when the fuel salt in the core becomes too hot, due to a number of reasons e.g. the breakdown of a pump. Also in this case, the freeze plug should melt to prevent the reactor from overheating. As the temperature in the reactor rises, pressure is also mounting, increasing the risk of an explosion.

The maximum temperature allowed in the reactor vessel is set at $T = 1200\,°C$, resulting in a maximum drainage time of approximately 8 minutes [8], assuming the MSFR's temperature is 700 °C.

In this thesis a new design of the passive freeze plug holder is examined, focusing on the freeze plug's melting behaviour in case of a station's black-out. The old and new design are shown in figure 1.3.

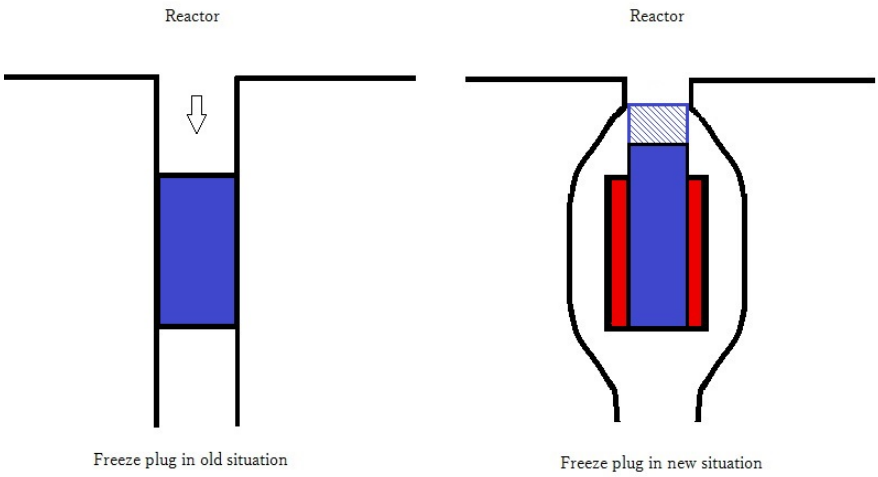

Figure 1.3: The vertical cross sections of two designs of the freeze plug. In the old situation, the pipe contains one frozen piece of salt, which has to melt all the way from top to bottom. As this takes too long [3], a new design is proposed, as shown on the right side.

The new freeze plug holder design is based on the advantages of melting by convective heat transfer from the sides of the plug. The freeze plug is extended to the smallest diameter of the pipe, shown as the shaded blue area. From there it is expected to melt first from the top, in the z-direction. As soon as the molten salt can flow past the solid salt, it will start heating up the thin metal ring (red) around the solid salt (blue). As a result, the solid salt plug will melt from the sides and is expected to fall down in due course, allowing for the remaining salt in the reactor vessel to flow down easily into the draining tanks.

1.4. Thesis outline

This thesis studies the expected behaviour of the new freeze plug holder's design with the goal to prove or to disprove its working principle by looking at the maximum allowed drainage time and the time it takes to drain the reactor vessel with this new design.
The theory behind the working principle of the safety plug is explained in chapter 2. Then, the modelling methods in COMSOL are described in chapter 3 and the results are listed and discussed in chapter 4. In the conclusion, the most important results are resumed and further research and possible new designs of the safety plug are proposed.

An overview of the used models is shown in table 1.1. The order of the models indicates the order of research that is done in this thesis.
The research question is: 'What is the emergency drainage time of the MSFR in case of station black-out with the new freeze plug holder design?'
To study this, three subquestions are posed:

- 'How does the freeze plug melt from the top?'
- 'When does the freeze plug fall down and how does convective heat transfer take place?'
- 'What is the drainage time of the reactor vessel when the molten salt can only flow past the plug through a narrow opening?' (for comparison with the melting time)

Table 1.1: Overview of the models in this thesis.

Model code	Purpose of model, determination of:	Solution method	Material	Program
1	Melting behaviour one-dimensional rod to check numerical method with analytical solution	analytically & numerically	water & salt	Matlab & COMSOL
2	Convective heat transfer, by modelling turbulent flow to visualize recirculation area's to determine appropriate Nusselt relations	numerically	salt	COMSOL
3	Radial melting behaviour freeze plug	numerically	water & salt	COMSOL
4	K-factor freeze plug when part of the freeze plug has melted from the top (narrow opening)	numerically	salt	COMSOL
5	Time to drain reactor vessel when part of the freeze plug has melted from the top (narrow opening)	analytically	salt	Matlab

2

Theory

In the freeze plug designed for the Molten Salt Fast Reactor (MSFR), different physical phenomena occur, which will be explained in the two sections of this chapter: one about all types of heat transfer and the physics that are needed for their determination and one about the drainage of the reactor.

2.1. Heat transfer

Three types of heat transfer occur in the freeze plug system, as shown in figure 2.1.

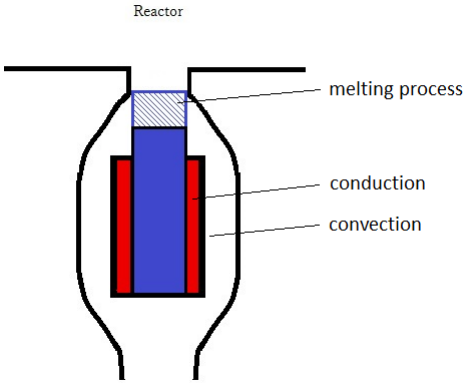

Figure 2.1: Freeze plug in its new holder design with the three heat transfer mechanisms shown.

Heat transfer with melting behaviour, conductive and convective heat transfer are explained in the following subsections. As a turbulence model is needed to determine the convective heat transfer, the theory behind this model is explained after the convective heat transfer subsection.

2.1.1. Heat transfer with melting behaviour

First, a general one-dimensional melting process is considered: a long rectangular rod of 'frozen' or solid salt, to which at the left end a certain temperature is applied. At $t = 0$, the melting process will start. The situation is pictured in figure 2.2.

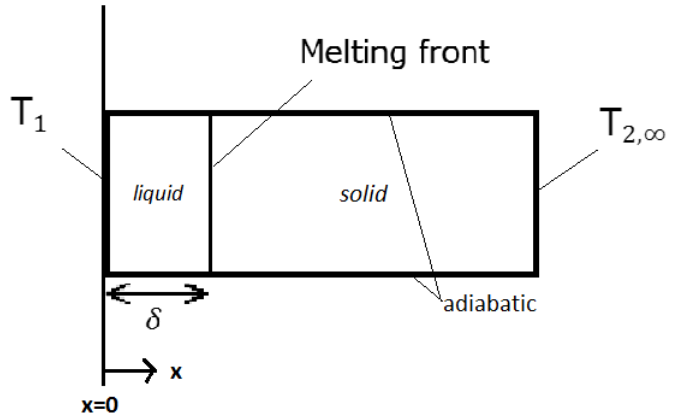

Figure 2.2: A long, solid rod to which a temperature T_1, higher than the melting temperature T_m, is applied on one side. $T_{2,\infty}$ is lower than T_m. This drawing shows a two-dimensional situation of the melting problem, but the calculation of the melting front is only done for the one-dimensional situation, which means that there is no temperature gradient in the vertical direction in this figure.

An energy balance is made at the melting front between the liquid and solid phase [3]:

$$\lambda_l \frac{\partial T(x,t)_l}{\partial x}\bigg|_{x=\delta} + \rho_s L_{fus} \frac{d\delta}{dt} = \lambda_s \frac{\partial T(x,t)_s}{\partial x}\bigg|_{x=\delta} \tag{2.1}$$

There are three terms in this differential equation. The first term (left) represents the conductive heat transfer in the liquid, the second term the heat consumed in the phase transition from solid to liquid and the third term the conductive heat transfer in the solid. Differential equation 2.1 can be solved for the temperature on the liquid and solid side using for example the Laplace method. The form of the solution of the temperature of the liquid is given in equation 2.2.

$$T_l(x,t) = T_l(x,0) + B\mathrm{erf}\left(\frac{x}{2\sqrt{\alpha_l t}}\right) \tag{2.2}$$

In equation 2.2 B is a constant. Imposing the condition that on the melting front at $x = \delta$ the temperature equals the melting temperature T_m and $T_l(x,0) = T_1$, we arrive at the following equation:

$$T_m = T_1 + B\mathrm{erf}\left(\frac{\delta}{2\sqrt{\alpha_l t}}\right) \tag{2.3}$$

Now a constant p is introduced: $p = \frac{\delta}{2\sqrt{\alpha_l t}}$, because the term in the erf function needs to be dimensionless. The value of B can be expressed in terms of p:

$$B = \frac{T_m - T_1}{\mathrm{erf}(p)} \tag{2.4}$$

Which brings us to the final expression of the temperature on the liquid side:

$$T_l(x,t) = T_1 + (T_m - T_1)\frac{\mathrm{erf}\left(\frac{x}{2\sqrt{\alpha_l t}}\right)}{\mathrm{erf}(p)} \tag{2.5}$$

On the solid side, a similar procedure is applied, which gives an expression for T_s of:

$$T_s(x,t) = T_2 - (T_2 - T_m)\frac{\mathrm{erfc}\left(\frac{x}{2\sqrt{\alpha_s t}}\right)}{\mathrm{erfc}\left(p\sqrt{\frac{\alpha_l}{\alpha_s}}\right)} \tag{2.6}$$

As $T_l = T_s = T_m$ on the boundary $x = \delta$, the equations for T_s and T_l are substituted in differential equation 2.1, resulting in the analytical solution:

$$\lambda_l \frac{T_m - T_1}{\sqrt{\pi \alpha_l}} \frac{\exp\left(-p^2\right)}{\mathrm{erf}(p)} + L_{fus} \rho_s p \sqrt{\alpha_l} = \lambda_s \frac{T_2 - T_m}{\sqrt{\pi \alpha_s}} \frac{\exp\left(-p^2 \frac{\alpha_l}{\alpha_s}\right)}{\mathrm{erfc}\left(p \sqrt{\frac{\alpha_l}{\alpha_s}}\right)} \tag{2.7}$$

Solving this equation, the value of p is determined, as this is then the only unknown parameter (the time-dependency drops out). With this value of p, the position of the interface can be calculated on any $t > 0$ with equation 2.8.

$$\delta(t) = 2p\sqrt{\alpha_l t} \tag{2.8}$$

In this calculation, several assumptions are made [3]:

- The properties of the liquid and the solid are constant and independent of the temperature. This is not the case in reality, but the assumption makes the partial differential equation easier to solve.
- The volume change due to phase change is neglected and so is the possibility of heat transfer by convection.
- The temperature T_1 on the side of the reactor vessel is constant.
- The melting point of the salt is constant. In reality, this is not the case for a binary system like the salt LiF-ThF_4.
- The plug is a semi-infinite medium, which is needed for the boundary conditions to make the differential equation easier to solve. In the MSFR, the freeze plug will have a finite length.

The melting behaviour is determined for both the water-ice system and the molten-solid salt by changing the applied properties, as will be explained in chapter 3.

2.1.2. Conductive heat transfer

Thermal conduction takes place in the material between the solid freeze plug and the turbulent flow of molten salt, as shown in the red area in figure 1.3. This material is hastelloy N, most commonly used in nuclear reactors [2].

Conduction relies on Fourier's law, which relates the heat flux to the temperature gradient [9] and is represented for a one-dimensional radial case by equation 2.9.

$$\phi''_{q,r} = -\lambda \frac{dT}{dr} \tag{2.9}$$

The term $\phi''_{q,r}$ is the heat flux on location r per unit area.

2.1.3. Convective heat transfer

Convective heat transfer takes place between the molten salt flowing past the plug and the solid material hastelloy N. Forced convection occurs, as the fluid flow is driven by gravity. The heat flux per unit area is decribed by 2.10.

$$\phi''_{q,r} = h \cdot (T_w - \overline{T}) \tag{2.10}$$

Where $\overline{T}$ is the mean temperature of the fluid and the heat transfer coefficient h is determined as in equation 2.11.

$$h = \frac{Nu \cdot \lambda}{D} \tag{2.11}$$

There are many relations for the Nusselt number for different geometries. In [4] this relation is experimentally determined for a cylinder in a turbulent axial flow for its three sides: top, bottom and axial side. It is assumed the function for Nu has a form of 2.12.

$$Nu = C \cdot Re^{e} \tag{2.12}$$

In which the parameters C and e depend on the location of the flow with respect to the cylinder and the configuration of the experimental setup. The Reynolds number is given in equation 2.13.

$$\mathrm{Re} = \frac{\rho v D}{\mu} \tag{2.13}$$

The characteristic length D is in this case of convective heat transfer the diameter of the freeze plug holder.

In the case where there is only a cylinder in a low upstream turbulent flow, the parameters in equation 2.12 for the three sides of the cylinder are given in table 2.1 [4]. For clarity, the different sides of the cylinder are drawn in figure 2.3.

Table 2.1: Parameters C and e in formula 2.12 for the Nusselt number of the heat transfer of a cylinder in an axial turbulent flow for different sides of the cylinder.

	C	e
top side	1.070	0.464
axial side	0.126	0.680
bottom side	0.122	0.642

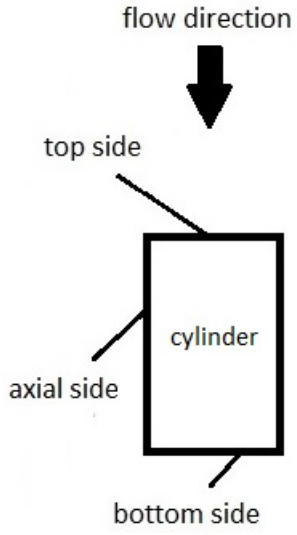

Figure 2.3: Cylinder in axial flow as described in [4]

Because the freeze plug with its holder do not have the same shape as the cylinder in figure 2.3, it needs to be checked if the fluid flows in the same way past the cylinder in figure 2.3 as past the freeze plug. The flow past the plug is numerically modelled as described in section 3.3.1. For this calculation, it is necessary to gain a better understanding of turbulence models, so in the next section the k-ϵ-model and its derivation are briefly described.

2.1.4. Turbulence model

For the design of the freeze plug, it is important to know how the fluid will flow through the pipe and around the freeze plug. For this purpose, the turbulent flow need to be calculated. First, it is necessary to determine the Reynolds number of the flow to check if the flow is

indeed turbulent. Though the properties of the molten salt are not accurately known, they are estimated to result in a Reynolds number well in the scope of turbulent flows, namely in the order of 10^5. The best way to describe turbulent flows is to numerically calculate the Navier-Stokes equations, but as this takes much time, data and computational power, models that simplify them are often used.

Most commonly used is the k-ϵ model, which is why it was also used in our simulation of the freeze plug. The k-ϵ model follows from the Reynolds equations in which one assumes that the relevant quantities like temperature, velocity, pressure and density can be described by an average value of the quantity plus a small perturbation. This kind of averages are called ensemble averages. [10]

$$\begin{aligned} \vec{v} &= \overline{\vec{v}} + \vec{v'} \\ p &= \overline{p} + p' \\ T &= \overline{T} + T' \\ \rho &= \overline{\rho} + \rho' \end{aligned} \tag{2.14}$$

When these equations are inserted in the Navier-Stokes equations, one arrives at the Reynolds Averaged Navier-Stokes equations (RANS) [11]:

$$\rho\left(\frac{\partial\overline{\vec{v}}}{\partial t} + \nabla\overline{\vec{v}}\right) = \rho\overline{\vec{g}} - \nabla\overline{p} + \mu\nabla^2\overline{\vec{v}} - \rho\nabla\overline{\vec{v'}\vec{v'}} \tag{2.15}$$

In RANS, the last term (right) is called 'Reynolds stress tensor' and comes from the turbulent eddies. It describes the momentum that is transported in the i-direction by turbulent fluctuations in the j-direction. This term is unknown and needs to be modelled by a closure model in order to have a sufficient number of equations to solve for all unknowns. The Boussinesq's closure hypothesis is used, where the Reynolds terms in RANS are described in the same way as molecular processes of viscous stress and heat conduction. The turbulent eddy diffusivity for momentum, ϵ_M, is introduced, so that the Reynolds term for momentum becomes [10]:

$$-\overline{\vec{v'}\vec{v'}} = \epsilon_M\left(\frac{\partial\overline{v_i}}{\partial x_j} + \frac{\partial\overline{v_j}}{\partial x_i}\right) \tag{2.16}$$

The eddy diffusivity for momentum ϵ_M can be modelled in different ways, of which one is the k-ϵ-model, where the transport of turbulence is taken into account. This transport can be described by the turbulent kinetic energy, $e = \frac{k}{\rho}$, and ϵ, the rate of dissipation. With the Kolmogorov relation an expression of the eddy diffusivity for momentum in both parameters e or k and ϵ of this model can be derived [10]:

$$\epsilon_M = C_\mu\frac{e^2}{\epsilon} = C_\mu\frac{k^2}{\rho^2\epsilon} \tag{2.17}$$

Where C_μ is an empirically obtained constant. The differential equations that describe the transport of k and ϵ have the same terms as those which occur in energy or momentum balances and are given in equations 2.18 and 2.19 [10]. The exact derivation of these differential equations is beyond the scope of this thesis.

$$\frac{\partial k}{\partial t} + v_i\frac{\partial k}{\partial x_i} = \frac{\partial}{\partial x_i}\left(\left(\nu + \frac{\epsilon_M}{\sigma_k}\right)\frac{\partial k}{\partial x_i}\right) + \rho\epsilon_M\left(\frac{\partial\overline{v_i}}{x_j} + \frac{\partial\overline{v_j}}{\partial x_i}\right)^2 - \rho\epsilon \tag{2.18}$$

$$\rho\frac{\partial\epsilon}{\partial t} + \rho v_i\frac{\partial\epsilon}{\partial x_i} = \frac{\partial}{\partial x_i}\left(\rho\left(\nu + \frac{\epsilon_M}{\sigma_\epsilon}\right)\frac{\partial\epsilon}{\partial x_i}\right) + C_{1\epsilon}\rho\epsilon_M\frac{\epsilon}{e}\left(\frac{\partial\overline{v_i}}{\partial x_j} + \frac{\partial\overline{v_j}}{\partial x_i}\right)^2 - C_{2\epsilon}\rho\frac{\epsilon^2}{e} \tag{2.19}$$

In these equations σ_k, σ_ϵ, $C_{1\epsilon}$ and $C_{2\epsilon}$ are constants with empirically obtained values:

Table 2.2: Constants in k-ϵ model.

Constant	Value
C_μ	0.09
$C_{1\epsilon}$	1.44
$C_{2\epsilon}$	1.92
σ_k	1.0
σ_ϵ	1.3

There are several possible programs that solve the k-ϵ-equations, using different assumptions. In this thesis the two-equation k-ϵ-model is used, as this is the most common one. Even though this model is not ideal for the geometry of the freeze plug [12], it is beyond the scope of this project to explore other types of models.

2.2. Drainage of the reactor

The drainage of the reactor will be explained only briefly in this report, because it is only relevant when comparing the melting time (time it takes to let the freeze plug drop down) to the time to drain the reactor once the molten salt can flow past the freeze plug holder. A more detailed study regarding the drainage of the reactor can be found in [13].

The drainage time of the reactor is calculated using an mechanical energy balance over the control volume, whichi is the volume of the reactor vessel plus the volume of the reactor pipe.

$$E_{tot} = E_{mechanical} + E_{thermal} \tag{2.20}$$

Because there is no energy production (steady state), no work done, a constant density and a constant mass flow, equation 2.20 looks like: [9]

$$0 = \frac{1}{2}({v_1}^2 - {v_2}^2) + g(z_1 - z_2) + \frac{p_1 - p_2}{\rho} - e_{fr} \tag{2.21}$$

The friction term e_{fr} consists of two parts, wall friction and friction due to pipe fittings or valves:

$$e_{fr} = 4f \cdot \frac{L}{D} \cdot \frac{1}{2}\vec{v}^2 + \sum_K \frac{1}{2}K\vec{v}^2 \tag{2.22}$$

The left part of this equation represents the wall friction and the right side represents friction due to the system design, i.e. the sudden contraction from the vessel to the drainage pipe and the freeze plug itself. The mechanical energy balance gives a differential equation for the height of the salt level in the reactor for time, which is solved in [13]:

$$h_{tank} = \frac{1}{4}\left(\frac{R_{pipe}}{R_{tank}}\right)^4 \left(\frac{2g}{1 + 4f\frac{L}{2R_{pipe}} + \sum K}\right) \cdot t^2 - \sqrt{H + L} \cdot \left(\frac{R_{pipe}}{R_{tank}}\right)^2 \sqrt{\frac{2g}{1 + 4f\frac{L}{2R_{pipe}} + \sum K}} \cdot t + H \tag{2.23}$$

Solving this equation for $h_{tank} = 0$ results in the drainage time.

3

Modelling in COMSOL

Because the melting behaviour of the freeze plug is quite complex, it has been modelled in different steps using the program COMSOL multiphysics as shown in table 1.1. The models that use COMSOL in table 1.1 are explained in this chapter.

3.1. Model 1: Melting behaviour one-dimensional rod

First, a one-dimensional model is used to verify if the model in COMSOL gives the same solution as the analytical one. As the analytical solution is calculated for a water-ice system, these materials are also used in the COMSOL model. The analytical solution is only calculated for the water-ice system and not for the molten-solid salt system, as its properties are better known. In section 3.2 more about the properties of the molten-solid salt is explained.

The geometry of the model consists of a straight line with a length of 0.2 m, which is twice the length of the investigated radius of the freeze plug of 0.1 m, and is used to ensure that penetration theory will hold for the set time span of 600 s, because the analytical solution is only valid for penetration theory. This is because a semi-infinite rod is considered at the analytical solution, so the heat flux will never arrive at the other side of the rod.

The physics module 'heat transfer in solids' is used with the following subfunctions:

- Initial values
- Temperature
- Thermal insulation
- Heat transfer with phase change

In 'initial values' the initial temperature of the material is set at $-20\,°C = 253\,K$. A high temperature of $50\,°C = 323\,K$ is applied to one end of the rod, while the other end is thermally insulated.
The 'heat transfer with phase change' module models the transition from one material to another, in this case from solid water (ice) to liquid water. In this module, the following properties of both materials need to be given: heat capacity, density, thermal conductivity, specific heat ratio, melting temperature, melting temperature range and latent heat of fusion. The melting temperature is set at 0 °C=273.15 K, the melting temperature *range* is changed to study its influence and the latent heat of fusion is $333 \times 10^3\,J\,kg^{-1}$ [6]. The other properties of solid and liquid water are given in table 3.1.

Table 3.1: Properties of solid and liquid water [6].

	solid water (253 K)	liquid water (323 K)
Heat capacity ($J\,kg^{-1}\,K^{-1}$)	$1.96 \cdot 10^3$	$4.18 \cdot 10^3$
Density ($kg\,m^{-3}$)	920.3	988.0
Thermal conductivity ($W\,m^{-1}\,K^{-1}$)	2.4	0.64
Specific heat ratio	1	1

A mapped mesh with a distribution function is used. With this function an explicit number of elements can be applied to one boundary. As this model has a one-dimensional geometry, the whole geometry is divided into a fixed number of elements. For research purposes, the number of elements has changed to study if the model gives different (and better) solutions for a smaller element size than for a relatively large one.

A time-dependent study is used, because we are interested in the position of the melting front and the temperature in the rod at different times. In addition, the temperature at the insulated side of the rod is measured to make sure that the rod is not yet heated through in the used time span, so that penetration theory is still applicable and the numerical solution can still be compared to the analytical one.
In this study module the constant Newton numerical method is used, which is explained in subsection 3.1.1. For stability the time stepping is said to be strict and the maximum time step is set at 1 second. This is done in order to prevent the model from stepping over the melting front during calculation. The speed of the numerical method needs to be smaller than the actual penetration velocity of the heat in the rod. The speed of the numerical method is approached with $\frac{\Delta x}{\Delta t}$, where Δx is the element size and Δt the time step.
Furthermore, the maximal order of the backward difference formula (BDF) method is set at 4 for stability. In this way the solution in COMSOL is more accurate and will be the same for every simulation.

3.1.1. Newton-Raphson method

The Newton(-Raphson) method is used for a good and stable numerical solution that does not require a too large computation time. It is used in all computations by COMSOL. The numerical method that uses equation 3.1 to find the root of the function $f(x)$ [14].

$$x^{k+1} = x^k - \frac{f(x^k)}{f'(x^k)} \tag{3.1}$$

This function is derived from the Taylor expansion:

$$0 = f(\xi) = f(x) + (\xi - x)f'(x) + O((\xi - x)^2) \tag{3.2}$$

In which the higher order term is neglected to arrive at formula 3.1. Figure 3.1 shows the undamped Newton method.

The tolerance determines the maximal value of k, that means that if condition 3.3 is met, the numerical calculation will stop. The tolerance is set at 0.1 in all COMSOL models used.

$$||f(u_k)|| < tolerance \tag{3.3}$$

Because calculating the inverse of the derivative takes up a lot of computation time, which can result in a non-converging simulation, a damping factor α is introduced. Instead of calculating the derivative in each point u_k and finding its root, the program now searches for a point u_{damped} where $f(u_{damped}) < f(u_k)$. u_{damped} is defined in the following way [15]:

$$u_{damped} = u_k + \alpha(u_{k+1} - u_k) \tag{3.4}$$

In all melting problem models in this thesis, the damping factor α is set at 0.9. The damped Newton method is shown in figure 3.2.

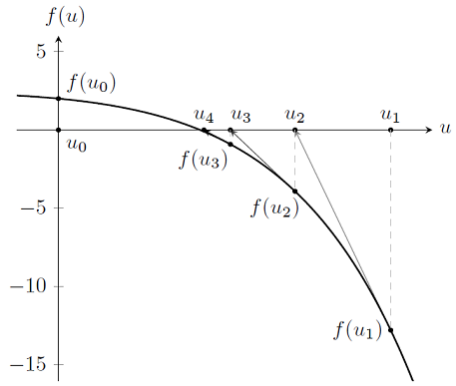

Figure 3.1: Newton method with starting point u_0.

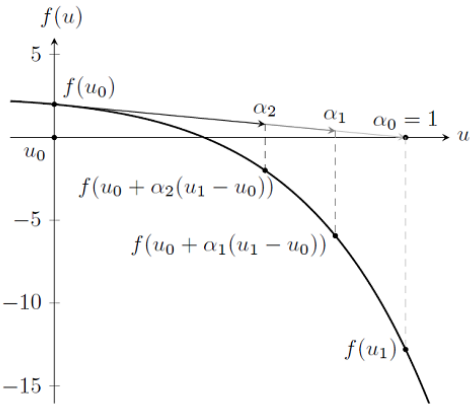

Figure 3.2: Damped Newton method with starting point u_0 and damping factors α_0, α_1 and α_2.

3.2. Implementation of the molten salt

In reality, the reactor is not filled with water, nor does the freeze plug consist of ice. To compare the melting behaviour of the water-ice system with the molten salt one, the previous model is also used to model the melting behaviour of the salt by using its properties.
However, very little is known about the physicochemical properties of this material and there are many different compositions of the salts. Ignatiev et al. investigated the properties of LiF-ThF_4 ($78 - 22$ mol %) for specific temperature ranges [16].

Table 3.2: Properties of molten salt LiF-ThF_4, where in all formulae temperature T is in K. The value of C_p for 700 °C is extrapolated, as it is out of the validity range.

	Formula	Value at 700 °C	Validity range (°C)
ρ (g cm^{-3})	$4.094 - 8.82 \cdot 10^{-4}(T - 1008)$	4.1249	[620 – 850]
ν (m^2 s^{-1})	$5.54 \cdot 10^{-8} \cdot \exp(3689/T)$	$2.46 \cdot 10^{-6}$	[625 – 846]
μ (Pa s)	ρ (g cm^{-3}) $\cdot 5.54 \cdot 10^{-5} \cdot \exp(3689/T)$	$10.1 \cdot 10^{-3}$	[625 – 846]
λ (W m^{-1} K^{-1})	$0.928 + 8.397 \cdot 10^{-5} \cdot T$	1.0097	[618 – 747]
C_p (J g^{-1} K^{-1})	$-1.111 + 0.00278 \cdot T$	1594	[594 – 634]

These properties are only valid for the liquid salt, because the melting temperature of the molten salt is 570 °C[17], which is below all validity ranges. For the solid salt, the properties are taken from the salt LiCl, whose melting temperature is close to the one of the molten salt, namely 610 °C [18]. Of course, this is rather a rough estimation of the molten salt's properties, bearing in mind we don't know whether these properties are the same for both salts, but since there is no information available yet on solid LiF-ThF_4($78 - 22$ mol %), an assumption is called for.
All necessary properties of LiCl are gives by the properties in the material database of COMSOL. Only the thermal conductivity of solid LiCl is not known in COMSOL, so this value is estimated by extrapolation of the formula in table 3.2, which gives a value of $\lambda = 0.99$. The other values are provided by the COMSOl database.

3.3. Model 2: Convective heat transfer model

This model consists of two parts. First the turbulent flow is modelled to determine to presence of recirculation area's. With this calculation, appropriate Nusselt relations are determined. In this section first the turbulence model is explained, after which a second model is mentioned. In this second model the influence of the different Nusselt numbers for the different sides,

as already explained in subsection 2.1.3, is studied.

3.3.1. Turbulence model

To determine the convective heat transfer around the from the molten salt to the freeze plug holder, the turbulent flow around the freeze plug is modelled in COMSOL.

This model uses the geometry shown in figures 3.3 and 3.4, as we are interested in the convective heat transfer when only 5 cm has melted from the top. This will be the geometry of the freeze plug system in the beginning of the emergency drainage process.

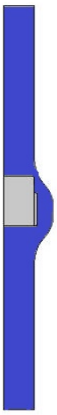

Figure 3.3: Two-dimensional axisymmetric model of the freeze plug with a pipe added before and after the plug part. In the model, the pipe before and after the freeze plug is made extra long in order to let the velocity profile recover from the freeze plug.

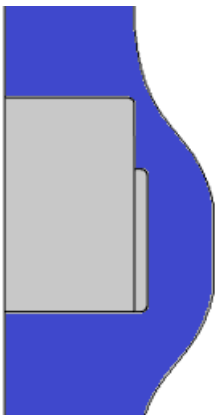

Figure 3.4: Zoom of freeze plug in figure 3.3, where 5 cm has melted from the top, so that the fluid can only flow between the solid plug and the wall.

In this model there are three domains, of which only the blue one is used, as the solid salt does not contribute to the turbulent flow, nor does the hastelloy N part. For the turbulent flow domain, the molten salt is used as material with the properties as given in table 3.2 for 700 °C.

The physics module 'turbulent flow, k-ϵ' is used to model the fluid flow. The k-ϵ model in COMSOL uses the same constants and properties as described in chapter 2.1.4, so the fluid is incompressible, the turbulence model type is RANS and the turbulence model itself is set at k-ϵ. The fluid is initially at atmospheric pressure and there is no velocity profile in the beginning. An inlet temperature is applied on the upper boundary to create a velocity profile. As different inlet temperatures are needed to determine the K-factor of the freeze plug system, this is explained more extensively in section 3.5.

The mesh settings are very important for computational fluid dynamics models, as there are many small vortices due to turbulence that need to be 'captured' in the mesh elements. This is why every model is first computed with a very coarse mesh to check if all settings are correct, before a finer mesh is applied. For the actual calculation, a physics-controlled mesh that is set at 'finer' is used, which gives a fine triangular mesh around the corners and turbulent points in the geometry as demonstrated by figure 3.5.

A stationary study module is applied, as we are only interested in the velocity profile and not specifically the turbulent flow on every time.
Finally, wall functions are applied on the wall, which are explained in the next subsection.

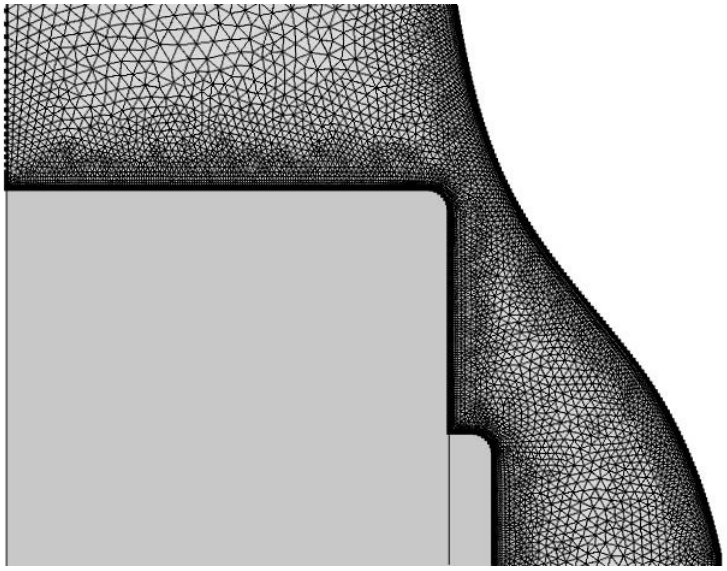

Figure 3.5: Free triangular finer mesh put on the geometry of which a zoom is made to the parts where the most complex turbulent flow occurs.

3.3.2. Wall functions

Wall functions are applied to the wall in the turbulence k-ϵ-model, as described previously. In short, wall functions describe the sublayers in the turbulent flow near the wall. Normally there are three sublayers: the viscous sublayer, the buffer layer and the log-law region. These three layers give a good estimation of the velocity profile near a wall. In figure 3.6 these three layers are shown.

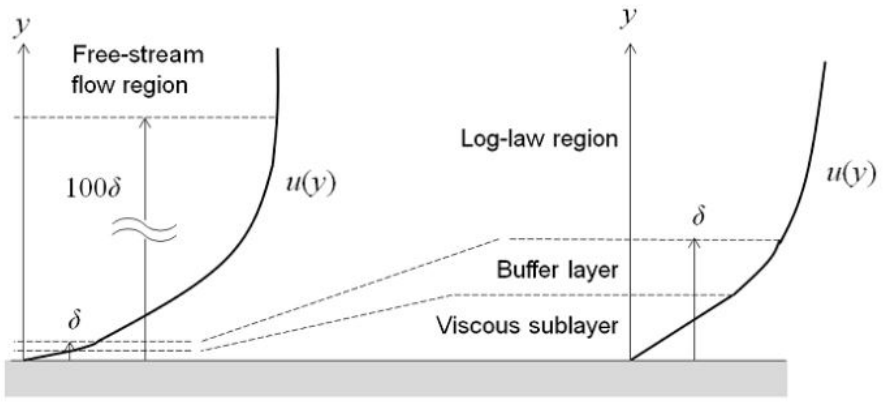

Figure 3.6: The velocity profile in a pipe (left) with a zoom on the wall region (right) [5]. Near the wall there are three layers: the viscous sublayer, the buffer layer and the log-law region. Each layer is described by another formula which cause different gradients to occur.

The wall functions module in COMSOL ignores the buffer layer and computes a nonzero velocity at the wall analytically [5]. This requires much less computation time than when the behaviour in the three layers is computed, but gives also a less accurate solution. For the goals in this thesis, wall functions are accurate enough, but in studying the heat transfer of the fluid to the solid plug, wall functions should not be used. The program must compute the fluid flow and heat transfer in the whole domain for a better result.

3.3.3. Influence Nusselt numbers on heat transfer

To visualize the influence of the three different Nusselt numbers (top, axial, bottom) for convection as described in section 2.1.3, a two-dimensional axisymmetric model is made, so

with (r,z)-coordinates. Three different heat transfer coefficients h are applied to the different boundaries: the top, axial and bottom boundary, as explained in figure 2.3. An image of the geometry is shown in figure 3.7.

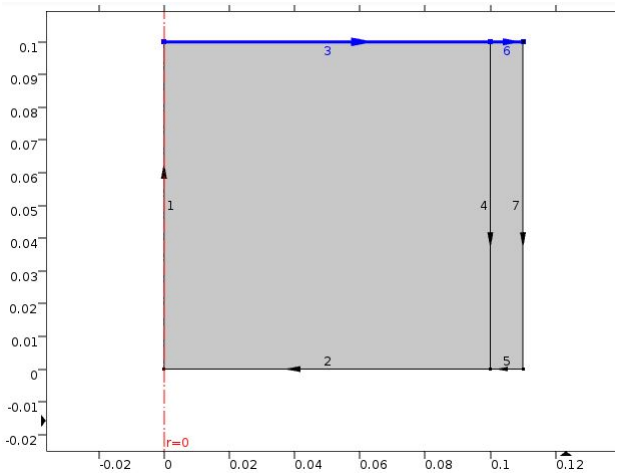

Figure 3.7: Two-dimensional axisymmetric model of the freeze plug and its holder in which the boundaries are indicated by a number. The right domain (rectangle) consists of hastelloy N and the left domain (square) consists of ice.

On boundaries 3 and 6 the top relation for Nu is used, on boundary 7 the axial relation for Nu and on boundaries 2 and 5 the bottom relation. The values of h for water are $2872,7286$ and 4160 $\mathrm{W\,m^{-2}\,K^{-1}}$ respectively. The remaining physics settings are the same as described in the previous section. For a more accurate calculation, the material of the freeze plug in this model is water.

A mapped mesh with a distribution is used for the whole geometry. On boundary 3 a distribution mesh of 500 elements is applied, on boundary 6 a distribution mesh of 50 elements and on boundary 7 there are 100 elements. This mesh is a around 10 times coarser than the one in model 1, but it requires already much more computation time. A zoom of the mesh is shown in figure 3.8. The model might not give a very accurate melting behaviour solution due to the coarse mesh, but it will visualize qualitatively the influence of the difference in convective heat transfer on the top, axial and bottom side of the freeze plug due to different Nusselt numbers.

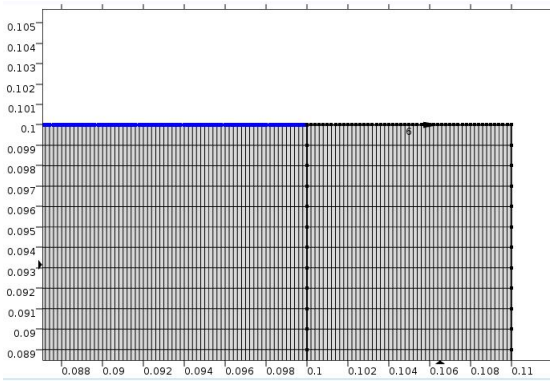

Figure 3.8: Zoom of the mapped mesh in the two-dimensional axisymmetric geometry shown in 3.7.

3.4. Model 3: Radial melting behaviour freeze plug

The freeze plug system has a radial geometry and a convective heat flux from three sides, the top, the sides and the bottom of the plug. For simplicity, the convective heat flux on the top and bottom are neglected, so the plug is modelled in a one-dimensional axisymmetric (radial) geometry. This geometry is shown in figure 3.10.
Next to the solid salt, there is a solid part made of hastelloy N, in which only thermal conduction takes place. Next to the hastelloy N part, the liquid flows past the plug, so that is the region where a convective heat flux occurs. This is shown in the two-dimensional axisymmetric model in figure 3.9.

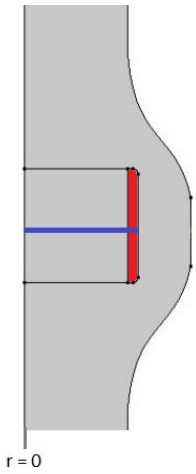

Figure 3.9: two-dimensional axisymmetric model of the freeze plug. The blue line represents the one-dimensional model as shown in figure 3.10. The red part is made of hastelloy N.

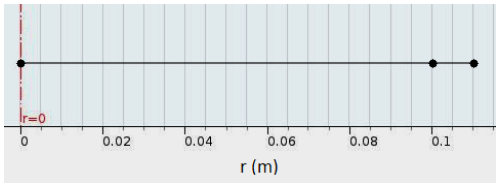

Figure 3.10: One-dimensional axisymmetric model of the freeze plug

As can be seen in figure 3.10, a line segment is added on the right of the line that represents the freeze plug. This line segment represents the hastelloy N freeze plug holder.
Two subfunctions are added to the physics model used in the subsection 3.1: 'heat transfer in solids' and 'heat flux'. The 'heat transfer in solids' is applied to the solid part of hastelloy N, in which conduction takes place. The properties of the metal holder, λ, C_p and ρ are given by the database of COMSOL.
Within the 'heat flux' function, one can model the convective heat flux that comes from the turbulent flow past the freeze plug. The heat transfer coefficient h and the temperature far away from the interface $T_{ext} = T_\infty$ are set. Although the temperature T_{ext} is in reality not far away from the interface and not constant in time nor position, an assumption is made that the temperature is constant and equal to 50 °C for the model with water and 700 °C for the model with the molten salt. The heat transfer coefficient h is calculated with the formulae described in subsection 2.1.3. Only the axial Nusselt relation is used, as the freeze plug is modelled in one dimension.

The model is used for both the water-ice system and the molten-solid salt system. The water-ice system is used again to check if the solution is similar to the expectations and if so, the molten-solid salt system is applied.
The used value of h for water is $7286\,\mathrm{W\,m^{-2}\,K^{-1}}$ and for molten salt $4160\,\mathrm{W\,m^{-2}\,K^{-1}}$. The difference is due to the different values of ρ and λ.

3.5. Model 4: Determination K-factor with turbulence model

The settings in this model are the same as described in section 3.3.1. The inlet boundary at the top of the pipe is given a fixed inlet velocity, that is increasing from $2\,\mathrm{m\,s^{-1}}$ to $6.5\,\mathrm{m\,s^{-1}}$ in steps of $0.5\,\mathrm{m\,s^{-1}}$ using a parametric sweep specified in the study module. Using different inlet velocities, one can determine the K-factor of the freeze plug, by computing the pressure difference over the plug and plotting it to the mean velocity of the fluid. The average pressure and velocity before and after the freeze plug are measured on red lines 1 and 2 in figure 3.11.

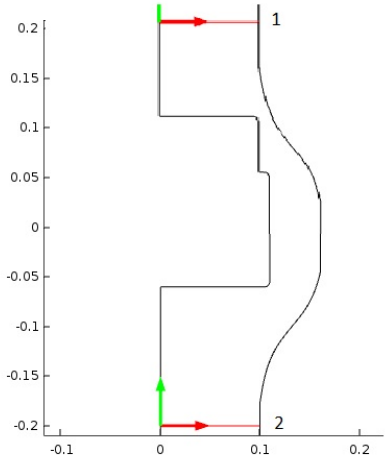

Figure 3.11: Two-dimensional axisymmetric model of the freeze plug, in which lines 1 and 2 are drawn. On these lines the average pressure and velocity are calculated.

With formula 3.5, the K-factor can be calculated by the use of a polynomial fit.

$$\frac{2\Delta p}{\rho} = K \cdot \overline{v}^2 \tag{3.5}$$

The outlet boundary is given a pressure condition, namely a pressure that is equal to the atmospheric pressure, assuming that the fluid can flow freely into the drainage tanks.

In the study module, a stationary solver is used with a parametric sweep for the velocity, as it considerably shortens computation time [13].

4

Results and Discussion

As mentioned in chapter 3, the emergency drainage process is modelled in different steps, which will be discussed separately in this chapter.

4.1. Model 1: Melting behaviour one-dimensional rod

With the modelling method described in chapter 3.1, the melting behaviour of the one-dimensional model of the water-ice system is determined in COMSOL. Later, a comparison of this melting behaviour of the water-ice system with the molten-solid salt system is made.

First, the influence of the different thermal conductivities of the two materials, ice and liquid water, is studied by looking at the temperature distribution in the rod, shown in 4.1.

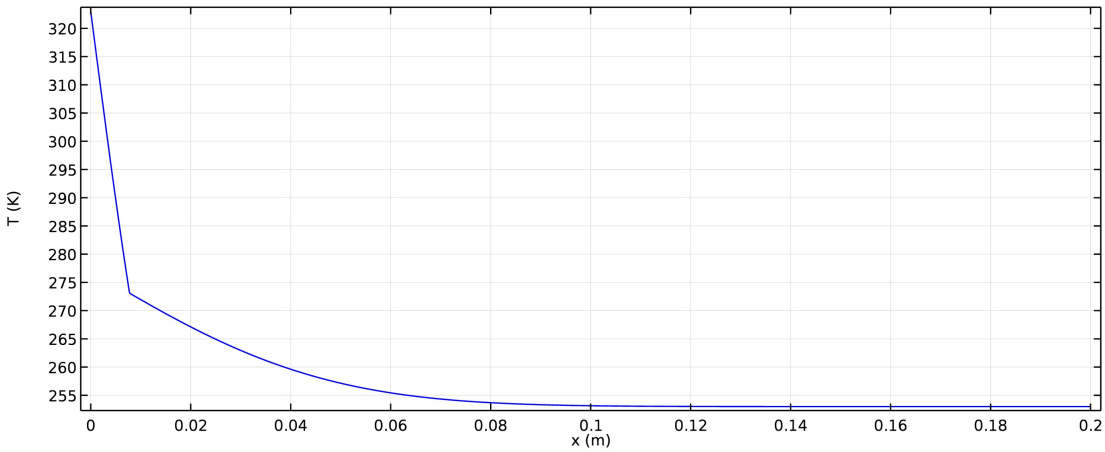

Figure 4.1: Temperature distribution at t = 300 s. The kink in the graph indicates the melting front.

This graph clearly shows the difference in thermal conductivity. The slope on the left side of the kink in the graph is much higher than the one on the right side. Besides, it also shows that the heat has not yet penetrated the entire rod, as the temperature on the right side of the rod at x =0.2 m is still at its initial value 253 K.

Secondly, a comparison was made of the melting time calculated in COMSOL and the one calculated analytically, for different melting ranges applied in the COMSOL model. The result is shown in figure 4.2.

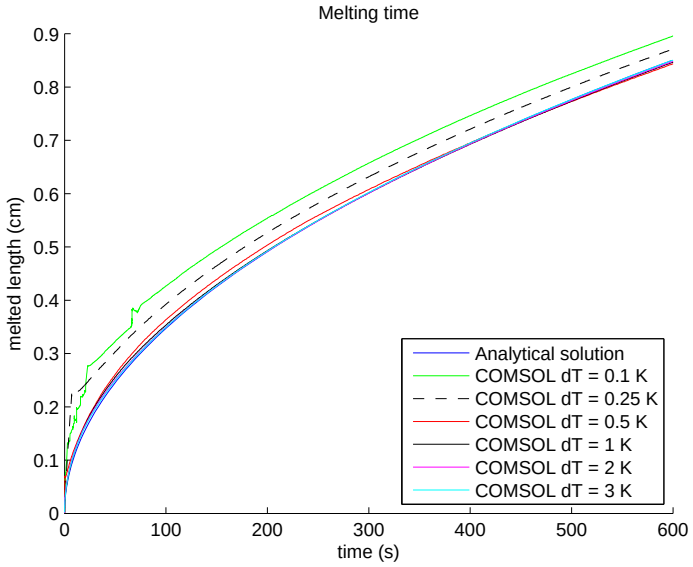

Figure 4.2: Melted length of the ice versus time for different melting ranges applied in COMSOL. The larger the melting range, the closer it approaches the analytical solution.

In the analytical solution, the melting range of the ice is 0 K, since it is considered a pure material. However, figure 4.2 shows that the larger the melting range, the more it resembles the analytical solution, whereas it is expected to behave the other way around. This can be caused by the fact that the computation of the phase change is harder for a small range, due to 'stepping over' the melting front during the calculation. This means that the width of the melting area where the liquid and solid phases are mixed, $T = T_m \pm 0.5 \cdot dT$, is smaller than the mesh element size. In this case, the numerical method does not 'see' this melting front with finite width. For a larger melting range dT, this is less likely to happen. The melting range 0.5 K is used for further calculations with the water-ice system, because it is close enough to the analytical melting range of 0 K and because the results of the melting problem model in COMSOL with this range are similar enough to the analytical solutioh.

With this melting range of 0.5 K the influence of the mesh size and the time step settings is determined using the same physics settings with different meshes or study configurations. This influence is shown in figure 4.3 of which a zoom is made and shown in figure 4.4.

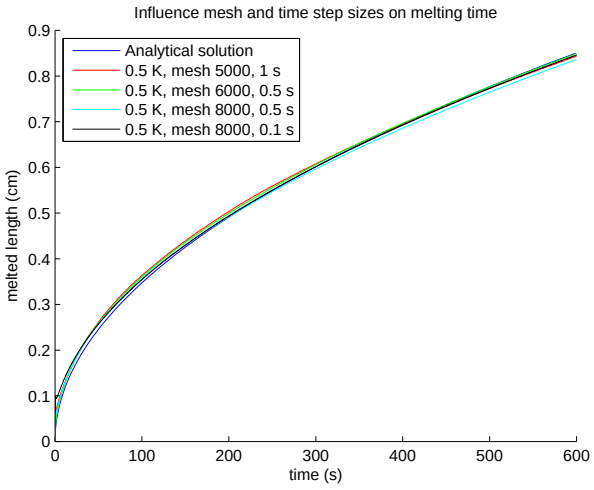

Figure 4.3: Melted length to time for different mesh settings. 'Mesh 5000' means that there are 5000 elements in the rod and the number of seconds in the legend represents the time step taken in the time-dependent solver.

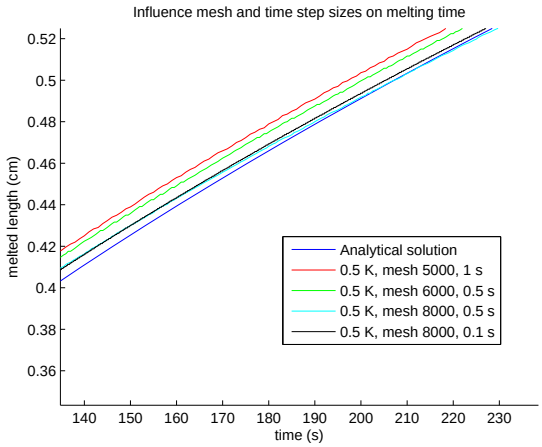

Figure 4.4: Figure 4.3 zoomed in for a better image of the differences between the solver settings. The finer the element size (the more elements in the mesh) and the smaller the time step taken in the solver, the more the modelled solution approaches the analytical one.

The melting behaviour of the water-ice system modelled in COMSOL is similar to the analytical solution, so the same model can be used for the properties of the molten-solid salt system in order to compare the melting behaviours of both systems. Of course these melted lengths cannot be easily compared with each other, as the systems are totally different. Note that the initial temperatures, the applied temperatures and the melting temperatures are different and the salt behaves as a binary system while water is a pure substance.
Because there is so little known about the molten salt, the melting range is set to be equal to the one of the water-ice system. The properties of the two systems are shown in table 4.1.

Table 4.1: Properties of the two melting systems.

	water-ice	molten-solid salt
Initial temperature solid $T_{s,i}$	−20 °C	500 °C
Initial temperature liquid $T_{l,i}$	50 °C	700 °C
Melting temperature T_m	0 °C	570 °C

With these settings and a mesh of 5000 elements and a melting temperature range of 0.5 K, the melted lengths at different times are plotted in figure 4.5.

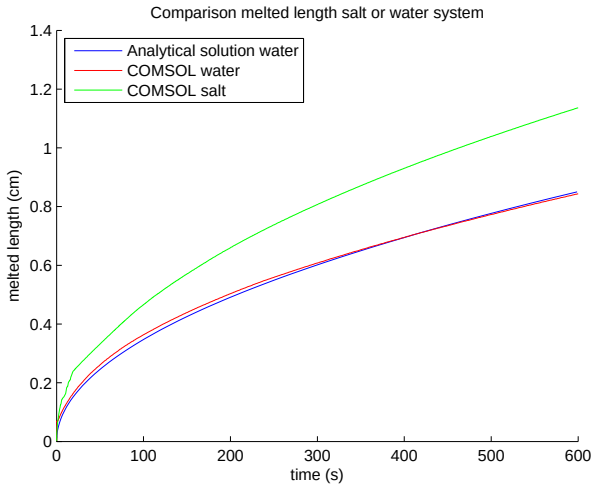

Figure 4.5: Comparison of melting behaviour of a one-dimensional rod between molten-solid salt system and water-ice system.

In figure 4.5, the analytical solution for the water-ice system is plotted to check the model in COMSOL. The analytical solution for the molten-solid salt system is not, since this would not make any sense as the analytical solution is only valid for a constant temperature and thus, a pure substance. Besides, C_p and ρ are dependent on temperature in the COMSOL model, while it is constant in the analytical model.
The molten-solid salt system shows a shorter melting time than the water-ice system in figure 4.5; during the same amount of time, a larger piece of the rod has melted. However, note that the properties of the salt are not very accurate, so further research is required to check if the chosen properties are valid. If they are not, the melting behaviour has to be checked using the adjusted properties.

4.2. Model 2: Convective heat transfer

The turbulent flow around the pipe has been calculated to describe the recirculation area's in the flow, to determine the different velocities through the pipe and to choose appropriate nusselt numbers. The influence of the different nusselt numbers for the convective heat transfer at different sides of the freeze plug is shown in the last subsection.

4.2.1. Turbulent flow

Direction of the flow

The direction of the flow is shown in figure 4.6 for an inlet velocity of $6.5\,\mathrm{m\,s^{-1}}$. The general flow direction is assumed to be the same for every inlet velocity.

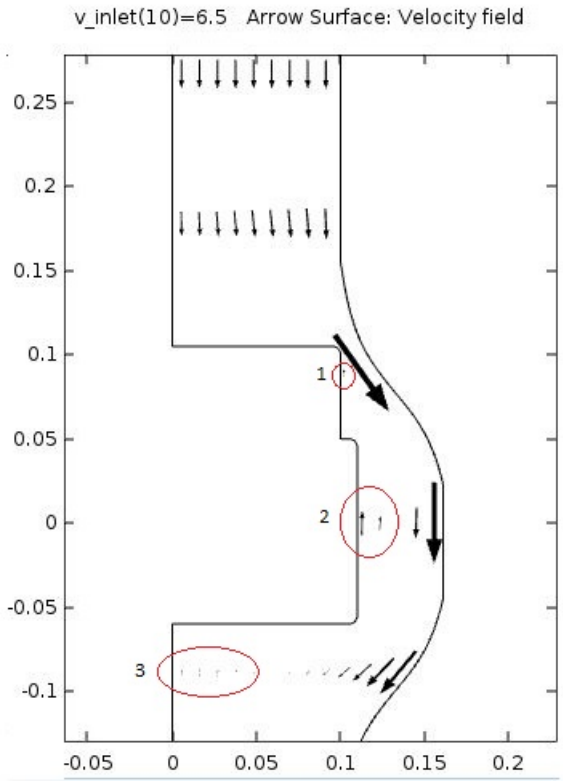

Figure 4.6: Turbulent flow in a two-dimensional axisymmetric model of the freeze plug. The direction of the arrows indicates the direction of the flow. The red circles indicate the recirculation areas.

There are three recirculation areas as can be seen in figure 4.6. A large one on the axial side of the plug (2), a small one next to the top of the axial side of the plug (1) and one at the bottom of the plug (3). The size of the arrows is proportional to the magnitude of the velocity, with a long and bigger arrow indicating a larger velocity than a small one. These recirculation areas are the same as expected and behave in a similar way as the ones around a cylinder in

an axial flow, which was used to estimate the Nusselt relations for convective heat transfer. Due to the same behaviour of the turbulent flow around an object, it is assumed that these Nusselt relations are valid for the freeze plug.

Velocities around the freeze plug

The inlet velocity is fixed in the turbulent model, but it is not constant in reality. The reactor vessel is emptying once the fluid can flow to the drainage tanks, which means that the body force due to gravity decreases as the amount of fluid in the vessel decreases. The velocity will decrease over time. As the velocity and exact drainage behaviour is beyond the scope of this thesis, the inlet velocity used in this model is 6.5 m s^{-1} is shown in figure 4.7.

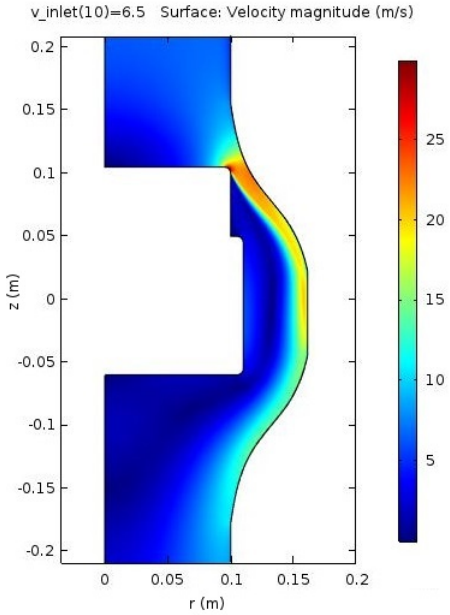

Figure 4.7: Turbulent flow in a two-dimensional axisymmetric model of the freeze plug. The velocity magnitudes of the turbulent flow for an inlet velocity of 6.5 m s^{-1} are indicated.

The velocity in the narrow opening is higher (20 m s^{-1}) than it initially is in the pipe (6.5 m s^{-1}), which is good for the heat transfer in that region. The fluid flow follows the pipe geometry which can be seen in the high velocity past the outer wall. Near the plug in axial direction, the fluid flow is slow, due to the recirculation area as described in the previous section. Even though the direction of the flow cannot be seen in figure 4.7, the velocity distribution also shows a recirculation area next to the plug, in zone 2. In the middle of the 'bypass' the fluid nearly stagnates, while the velocity is higher near the axial wall of the plug. This indicates that in the middle, the fluid changes direction and near the axial wall it flows back upwards with a higher speed.

4.2.2. Influence Nusselt numbers on heat transfer

The influence of the three different Nusselt numbers (top, axial, bottom side) is studied and modelled for the water-ice system. This system is used instead of the molten-solid salt system, as we are only interested in the influence of the Nusselt numbers. Because the properties of the water-ice system are more accurate, this will give a better numerical solution.
The mesh is coarser than the one used in the one-dimensional model, so the temperature distribution is expected to not be very accurate. The goal of this model is to show the difference in Nusselt relations and heat fluxes on the different boundaries.

The isothermal contours of the temperature in the freeze plug are shown for time t=300 s in figure 4.8.

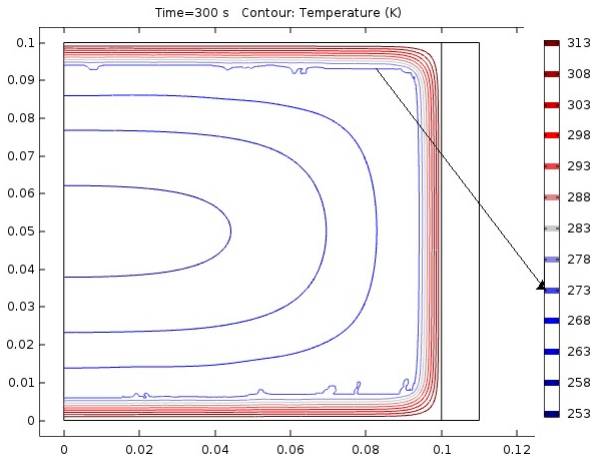

Figure 4.8: Isothermal contours in freeze plug for t=300 s. Different heat fluxes have been applied on the top, axial and bottom boundaries. The melting front with T = 273.15 K is indicated extra clearly by the arrow.

The heat is expected to penetrate further into the ice block from the bottom than from the top, as the heat flux is higher on the bottom boundary. However, this is not demonstrated by figure 4.8. Most likely, this is because the mesh is too coarse. This influence is also visible in the small bumps in the contours. In these bumps, the coarse mesh or the too large time step 'jumped' over the melting front, such that the melting front can not be determined accurately anymore. A finer mesh and smaller time steps in the settings are expected to show the difference in heat fluxes on the boundaries.

4.3. Model 3: Radial melting behaviour freeze plug

The next step in the modelling process is the radial melting process in the freeze plug, where the hastelloy N ring and the heat flux are added, as described in section 3.4. The melting behaviour of the water-ice system for different settings in this model is shown in figure 4.9. Again, first the water-ice system is considered to verify the melting behaviour solution of the numerical method.

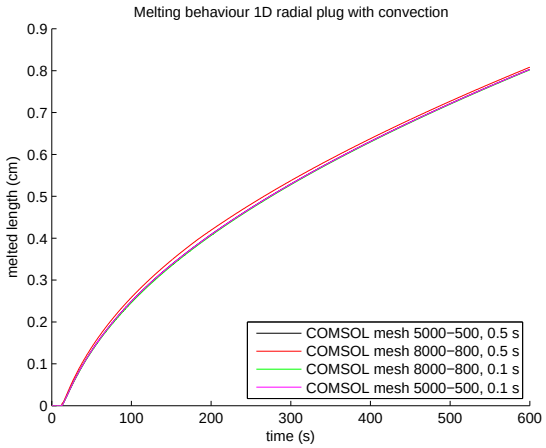

Figure 4.9: Melting behaviour of one-dimensional radial freeze plug with hastelloy N wall and forced convection for the water-ice system. In this figure the melted length has been plotted for different settings of the element size in the mesh and the time step taken by the solver.

The different mesh settings give almost the same solution for the melted length, so less computationally expensive settings can be used for further calculations. Furthermore, the melting behaviour of the one-dimensional radial plug with the hastelloy N ring and convective heat transfer is compared to the melting behaviour of the one-dimensional radial plug with-

out the metal part and convection, so only with an applied fixed temperature on the right boundary of the ice to show the influence of the forced convection. This last case can be compared with the heat transfer coefficients of the hastelloy N ring and the convective heat transfer approaching infinity, such that the heat transfer resistance approaches zero. This influence can be seen in figure 4.10.

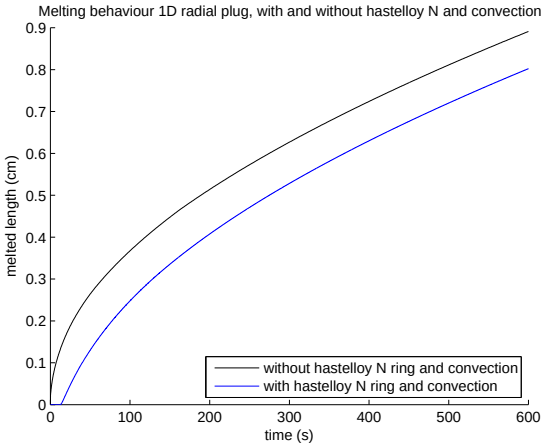

Figure 4.10: Comparison of the melting behaviour of a one-dimensional radial plug with and without the hastelloy N wall and forced convection for a mesh of 7000 elements and a time step taken of 0.5 s for the water-ice system.

In figure 4.10 it is clear that there is a *horizontal* offset of the melting process, which is caused by the fact that it takes some time for the heat to reach the frozen plug. The heat has to pass the hastelloy N ring first before it starts melting the plug. Apart from that, the shape of the two graphs is quite similar, which makes sense as the penetration of the heat in the frozen plug is the same with or without convection, as the heat flux is constant once the heat from the liquid has reached the 'frozen' salt.

The melting behaviour of the one-dimensional radial plug is investigated with water only, as its properties are more reliable than the ones of the molten salt. However, here again, a comparison of the molten-solid salt system and the water-ice system is made to determine the expected melting time of the freeze plug of molten salt. This is shown in figure 4.11.

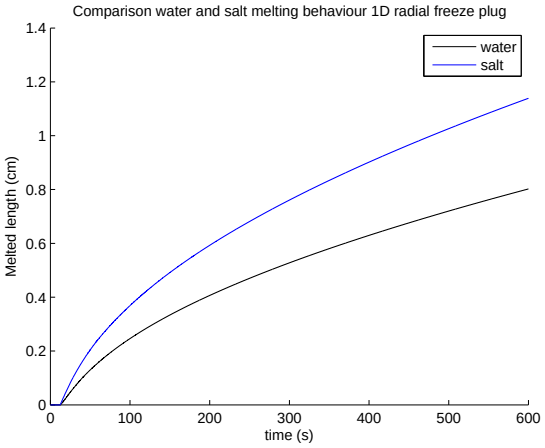

Figure 4.11: Comparison of the melting behaviour of the molten-solid salt system and the water-ice system for a model of a one-dimension radial plug with a hastelloy N wall and forced convection for a mesh of 8000 elements and a time step of 0.1 s.

The molten-solid salt system gives a smaller melting time than the water-ice system, as can been seen in figure 4.11. Besides, the offset of the melting behaviour of the salt is a

little smaller, as the heat transfer coefficient h is higher for the salt than for water due to different physicochemical properties. The penetration of heat goes faster through solid salt than through ice, as shown in figure 4.5. These two phenomena cause the freeze plug made of solid salt to melt faster than the freeze plug of ice.

4.4. Model 4: Determination of the K-factor

The K-factor is determined as described in chapter 3, so the pressure and velocities are calculated just before and just after the plug [13].

In Matlab the pressure difference between the two line averages over the density is plotted to the mean velocity of both line averages. This gives the following result:

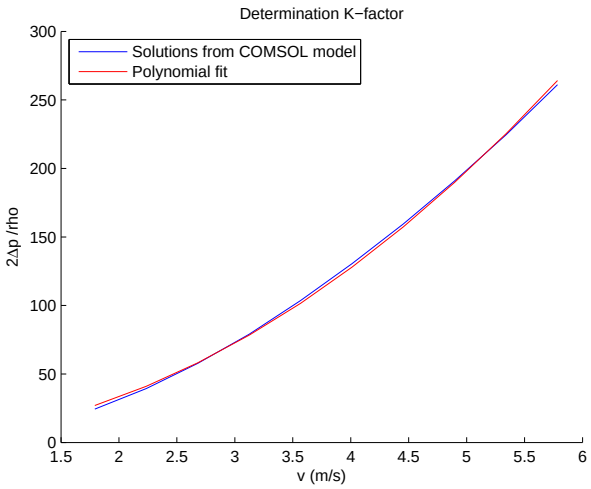

Figure 4.12: Determination of the K-factor, by applying a polynomial function to the solution generated by the model in COMSOL.

For the calculation, a first order polynomial fit is made for v^2 to $\frac{2\Delta p}{\rho}$ of the form: $\frac{2\Delta p}{\rho} = a \cdot x + b$ with a and b constants and $x = v^2$. This linear function is then plotted for v in this figure, what makes the fit function of the form of $\frac{2\Delta p}{\rho} = av^2 + b$. Constant a in the polynomial fit is equal to the K-factor, which gives a value of 7.84. This is a plausible value, as the order is correct and it is higher than the ones found for the freeze plug when it is melted further, which makes sense as the fluid has a narrower opening to flow through than in the calculations in [13].

4.5. Model 5: Time to drain reactor vessel when a part of the freeze plug has melted from the top

With this K-factor an estimate is made of the time needed to empty the reactor vessel when only the freeze plug has only melted 5 cm from the top, hereafter called 'drainage time'. In reality the size of this opening increases over time, but as it takes too much computation time to model this time-dependent behaviour, the drainage time is calculated for a fixed opening. This drainage time is an estimate to compare with the radial melting time that is described in the next section.

The drainage time is calculated using formula 2.23. To model the volume of the molten salt in the whole reactor system, the modelled vessel is larger than the actual one, because the volume of the pipes is included in the vessel volume. This results in a vessel height of 2.84 m with a radius of 1.42 m [13], assuming the vessel has the same diameter and height. The Fanning friction factor f is equal to 0.0034 [13] and the length of the pipe is estimated to be 1.33 m, which is also used in the COMSOL model. This length is used in equation 2.23

in the square root factor $\sqrt{H+L}$.
For the other L-term in equation 2.23, the $4f\frac{L}{D}$-term, a different length is taken for the following reason. This L-term represents the length of the entire pipe and is needed to determine the friction caused by the wall. As all friction in the freeze plug area, i.e. between the two horizontal lines in figure 3.11, is represented in the K-factor, the wall friction of this pipe length must not be included in the $4f\frac{L}{D}$-term, to prevent the wall friction from being taken into account twice.

The measures of the system are shown in figure 4.13.

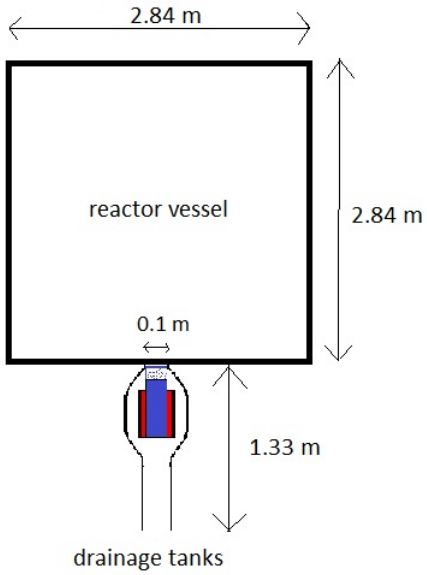

Figure 4.13: Schematic representation of the reactor system. Note that the reactor vessel has the modelled dimensions and not the actual ones. The image is not to scale.

With these settings and values of the constants in equation 2.23, figure 4.14 of the height of the liquid in the reactor vessel is made.

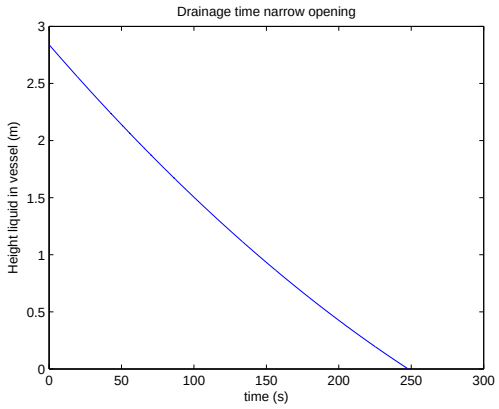

Figure 4.14: The course of the height of the liquid in the modelled reactor vessel, starting with a full vessel of height 2.84 m.

In this figure, the fact that the freeze plug immediately starts melting and that the fluid starts flowing through a narrow opening before this opening reaches the 5 cm width considered in this model, is not taken into account. With all these assumptions the reactor vessel is expected to be empty after approximately 250 s.

4.6. Emergency drainage time

The total emergency drainage time consists of three parts as shown in equation 4.1.

$$t_{drain,tot} = t_{melt,top} + t_{drop} + t_{drain,rest} \tag{4.1}$$

In this equation $t_{drain,tot}$ represents the total emergency drainage time, that is the time from the first moment there is a station black-out to the moment when all molten salt has flown to the drainage tanks. The determination of the other three times is explained the the following subsections.

4.6.1. Determination $t_{melt,top}$

In case of station black-out, the freeze plug has to melt first in the vertical direction (linearly) before the warm fluid can flow past the plug and melt it from the sides.

The turbulent flow is simulated for a melted length of 5 cm from the straight part of the pipe to the top of the solid salt. Melting 5 cm is not realistic, because it will take longer than 8 minutes, as can be seen in figure 4.5. However the slope of the narrowing part of the plug can be made less steep in order to decrease the distance from the straight pipe to the top of the solid plug. This can be reduced to 1 cm. This adjustment is visualized in figure 4.15.

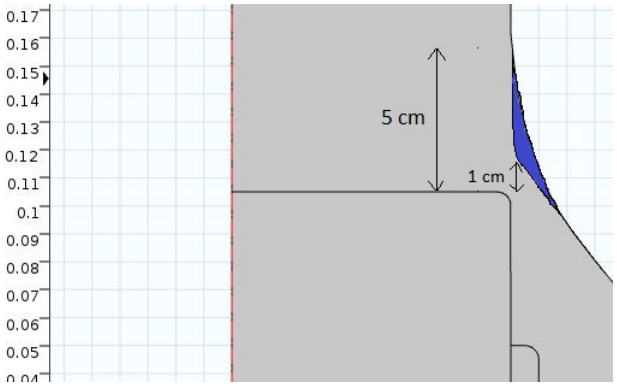

Figure 4.15: Adjusted design for the freeze plug in order to reduce the linear melting time from the top. The blue part is removed to make the distance between the straight pipe (the top of the solid part in the beginning) and the top of the solid part once it has melted smaller. The necessary length to melt from the top is reduced from 5 cm to 1 cm.

Concerning the initial linear melting behaviour of the top of the frozen plug, we need to look at the melted length needed for the liquid salt to flow past the plug. The exact melting behaviour of the top of the plug is not investigated in this thesis, but it is estimated that a melted length in the z-direction of 5 mm is enough to let the liquid salt flow past the plug and start the convective heat transfer process. It takes 115 s to melt 5 mm from the top as can be seen in figure 4.5, so $t_{melt,top}$ =115 s. A melted length of 5 mm is not much, but it is expected that the solid plug will melt faster from the sides once the warm fluid flows through the small opening, allowing for a conductive heat transfer.

4.6.2. Determination t_{drop}

t_{drop} is the time it takes the freeze plug to drop down. There is no information available yet what thickness needs to melt from the sides before the solid salt drops down, but it is estimated to be 2 mm, as there is then a small liquid layer between the hastelloy N ring and the solid salt cylinder. The gravity force of the molten salt in the reactor vessel will push the plug down. Less than 2 mm seems unlikely, as it is expected that the plug will not melt perfectly uniformly, due to e.g. imperfections in its structure.
This will take 50 s, as can be seen in figure 4.10, so t_{drop} =50 s.

Together with $t_{melt,top}$, the frozen plug is expected to drop after 165 s. The uncertainty in this melting time is hard to determine quantitatively, as it is not known what the deviation

of the properties of the liquid salt and solid salt are with respect to the real ones and the uncertainty in the simulation of the COMSOL models is not known.

4.6.3. Determination $t_{drain,rest}$

Once the frozen plug has dropped down, the remaining molten salt has to flow to the drainage tanks. Assuming the reactor vessel is full, this will take 80 s, so $t_{drain,rest}$ =80 s [13]. However, the reactor vessel is not full, as a part of the fluid has already flown down into the drainage tanks making the drainage time less than 80 s. How much less is not known, as it is not determined in this thesis what the flow rate past the freeze plug over time is.

4.6.4. Total emergency drainage time

The three determined times $t_{melt,top}$, t_{drop}, $t_{drain,rest}$ are filled in in equation 4.1:

$$t_{drain,tot} = 115 + 50 + 80 = 245\,\text{s} \tag{4.2}$$

The emergency drainage time of 245 s is the maximum value as $t_{drain,rest} \leq 80$ s. This time is below the maximum permitted emergency drainage time of 480 s[8], meaning it is perfectly admissible. As mentioned before, the uncertainty in this time cannot be determined quantitatively, but its value is almost half the permitted emergency drainage time, so it can be concluded that the new design of the freeze plug holder might work.

Besides, the time it takes to drain the reactor vessel when a part of the freeze plug has melted from the top is compared to the time till the freeze plug has dropped down. If the reactor is already drained before the freeze plug has dropped down, the design of the freeze plug holder might be reconsidered. However, the time it takes to drain the reactor when a part of the freeze plug has melted (model 5) is 250 s, while only 115 s passed before the freeze plug fell down. This confirms the good working principle of the new design of the freeze plug holder.

5

Conclusion

The melting behaviour of the freeze plug in a molten salt fast reactor is explored in this thesis. Several aspects of the plug are studied, after which an emergency drainage time is determined. This time consists of three parts: the time needed for the top of the plug to melt in order to let the molten salt flow past the plug, the time the freeze plug needs to drop down due convective heat transfer from the sides and the time it takes to drain the molten salt in the reactor vessel once the freeze plug has dropped down. These times add up to an emergency drainage time of 245 s, which is less than the maximal allowed drainage time of 480 s. This design of the freeze plug might work.

However, further research will be needed to give a more accurate value of the melting time. In this thesis, the physicochemical properties of the solid salt have been estimated using those of another salt. It is not certain that LiF-Th_4 will behave in the same way. Besides, the different melting behaviours (from the top and from the sides) need to be combined into one model, so that the melting behaviour of the whole plug and the fluid flow can be determined for every time step. The importance of these unknown factors cannot be quantitatively expressed in an uncertainty of the melting time, so that is why only a value of the melting and drainage time are given. The conclusion that this design might work can still be drawn, as the determined drainage time is almost half the permitted drainage time.

5.1. Recommendations

During this research many aspects of the melting behaviour and the freeze plug came along and most of them were beyond the scope of this thesis. However, the required K-factor and the turbulent flow have been examined, even though they were not part of the original plan. Aspects that still require further research are:

- The properties of the molten salt have only been researched once and additional research is needed for a more accurate estimate. Furthermore, the physicochemical properties of the solid salt are unknown, calling for research as well.

- The Nusselt relations of the convective heat transfer are assumed to be the same as convective heat transfer around a cylinder in a free flow. However the freeze plug cylinder does not have a free flow around it, but a flow bounded by walls. A more accurate Nusselt relation must be determined by either experiments or an analytical setup.

- The melting behaviour of the solid plug in the beginning of the melting process needs to be investigated, as the plug does not only melt linearly, in the z-direction, but also in the r-direction once the fluid can seep through the small opening. When the fluid flows through this aperture, it is expected that it will make the solid salt melt faster due to friction and convective heat transfer.

- The time-dependent behaviour of the solid plug initially melting from the top and the fluid flow must be combined into one model. In this way the radial melting behaviour of the plug due to convective heat transfer from the sides is recorded from the very moment the fluid starts flowing past the cylinder and not after the top has melted 5 mm. Besides, in this model the amount of molten salt that flows into the drainage tanks must be calculated. In this way it can be determined if the vessel is already drained before the freeze plug has dropped down.
- Research is needed to determine how the solid plug can extend to the straight pipe first when there are no cooling elements around it. The part of the solid salt in the freeze plug, which is surrounded by hastelloy N, can be cooled by a heat exchanger in the metal part, but the solid salt on top of this plug is not cooled in this model.
- The freeze plug just floats in the widening part of the pipe now, which is technically not possible. A system of supporting bars will be needed to keep the hastelloy N ring in its place. These bars have an influence on the turbulent flow, which must be examined.
- The pipe narrows after the freeze plug, which has no actual function. This model is just used for an initial exploration. In further research the freeze plug can be modelled with a straight, broad pipe to the drainage tanks, which is expected to be better, as the freeze plug cannot block the pipe while falling down.
- Research into the forces on the freeze plug is needed to check if the freeze plug stays in its place when it is cooled to 500 °C. The molten salt in the reactor vessel presses on the freeze plug, so a strong friction force is needed for the plug to 'stick' to the hastelloy N ring instead of being pushed down. A lower temperature might be needed or maybe a higher pressure below the plug to reduce the pressure difference between the top and the bottom of the freeze plug.
- The influence of the temperature of the molten salt as it flows past the plug is yet unknown, as hastelloy N and solid salt are cold. A layer of solidified salt may occur on the outer wall of the hastelloy N ring.

5.1.1. Other designs for the safety plug

During this project, different designs have been thought of should this design of the freeze plug not work. Even now this preliminary study shows that the design might work, two other concepts are shortly explained. These plug designs, based on different physical phenomena, are called the break plug and the mechanical plug.

The break plug

The concept of the break plug is based on the higher pressure encountered by the top of the plug. This pressure can be maintained by applying an equally high pressure below the plug, in such a way that the forces on the plug from top and bottom cancel each other out and the resulting force in vertical direction equals zero.
The high pressure below the plug is maintained by a pump, that works on electricity. When there is a station black-out, the pump will stop working, so the high pressure below the plug will fall away. The plug, or better called diaphragm, will break and the molten salt will flow down into the drainage tanks.
The other case in which the safety plug must stop operating, is when the temperature in the reactor vessel is a critical level. This is harder to achieve passively with the break plug. A temperature sensor could be placed above the plug triggering the pump to stop working as soon as the temperature has reached a certain level.
This is just a very basic design that still requires quite some additional research.

The mechanical plug

A mechanical plug is actually not a preferable option, as it needs to operate passively in order to serve as safety measure. However, this requirement is met if the mechanical plug only functions as a plug in case there is electricity available.

Such passive behaviour can for example be established by a magnetic plug that is held by an electromagnet, which only produces a magnetic field when an electric current flows through the wires. This means that the magnetic plug will fall down if there is a station black-out, so it meets the first requirement. Research is needed as to what materials can be used for the magnetic plug and how leakage can be avoided.
The other circumstances, temperature reaching a critical level, can be addressed with a temperature sensor, as described in the previous subsection.

The two designs are shown in figure 5.1

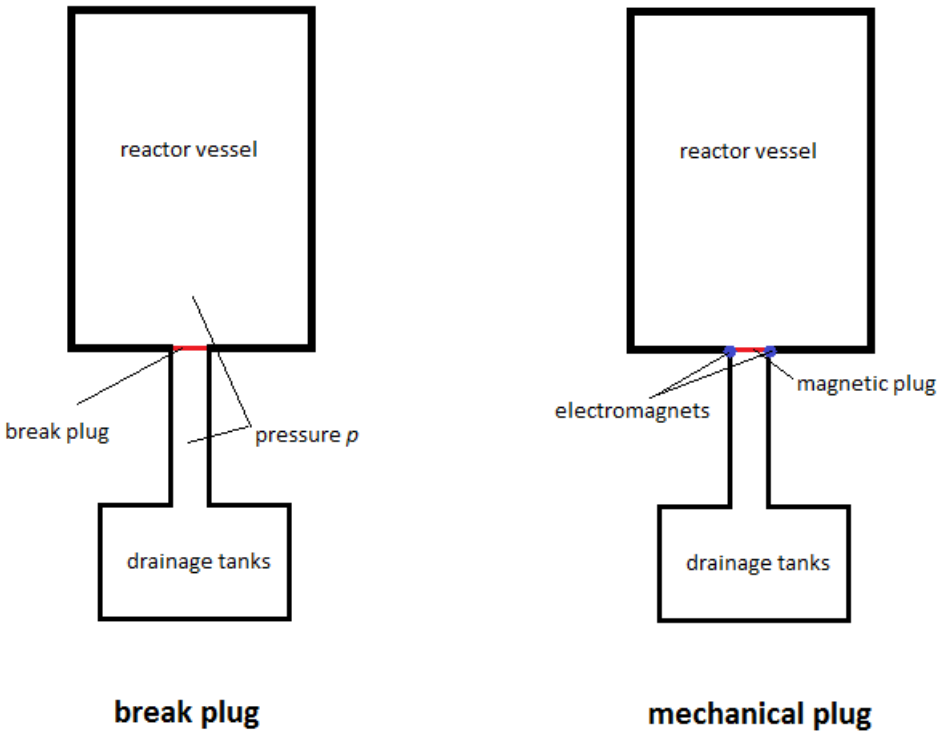

Figure 5.1: Two new conceptual designs of the safety plug: the break plug and the mechanical plug.

Bibliography

[1] J.-L. Kloosterman, *Nuclear reactors, generation of reactors,* http://www.janleenkloosterman.nl/reactors.php.

[2] J. Serp *et al.*, *The molten salt reactor (msr) in generation IV : Overview and perspectives,* Elsevier **77**, 308 (2014).

[3] P. Swaroop, *Design of a Freeze Plug for the Molten Salt Reactor (MSR)*, System integration project, Delft University of Technology (2015).

[4] R. Niberg and N. Lior, *Convection heat transfer coefficients for axial flow gas quenching of a cylinder,* in *Proceedings of the Fourth International Conference on Quenching and the Control of Distortion* (Beijing, 2003).

[5] W. Frei, *Which turbulence model should I choose for my CFD application?* https://www.comsol.com/blogs/which-turbulence-model-should-choose-cfd-application/ (2013).

[6] D. R. Lide, *CRC Handbook of chemistry and physics*, 82nd ed. (CRC Press LLC, Boca Raton, Florida, 2001).

[7] Y. Amano, *The Fukushima Daiichi Accident*, Tech. Rep. (International Atomic Energy Agency, 2015).

[8] M. Brovchenko, D. Heuer, E. Merle-Lucotte, M. Allibert, V. Ghetta, A. Laureau, and P. Rubiolo, *Design-related studies for the preliminary safety assessment of the molten salt fast reactor,* Nuclear Science and Engineering **175**, 329 (2013).

[9] R. Mudde and H. van den Akker, *Fysische Transportverschijnselen*, 4th ed. (Delft Academic Press, 2014).

[10] M. Rohde, *Nuclear reactor thermal hydraulics (AP3641),* (2014).

[11] R. B. Bird, W. E. Stewart, and E. N. Lightfoot, *Transport Phenomena*, 2nd ed. (John Wiley & Sons, 2002).

[12] S. Hickel, *Reynolds averaged Navier-Stokes,* University Lecture TU Delft (2016).

[13] O. C. van den Bergh, *Emergency drainage of the MSFR*, Bachelor thesis, Delft University of Technology (2016).

[14] J. van Kan, A. Segal, and F. Vermolen, *Numerical Methods in Scientific Computing*, 1st ed. (VSSD, 2008).

[15] W. Frei, *Solving nonlinear static finite element problems,* https://www.comsol.com/blogs/solving-nonlinear-static-finite-element-problems/ (2013).

[16] V. Ignatiev *et al.*, *Progress in development of MOSART concept with Th support,* (2012).

[17] S. Phapale, A. N. Shirsat, *et al.*, *Determination of eutectic composition and heat capacities of fuel salt and blanket salt mixtures,* in *Proceedings of Thorium Energy Conference 2015* (Mumbai, India, 2015).

[18] M. M. Kenisarin, *High-temperature phase change materials for thermal energy storage,* Elsevier **14**, 955 (2010).

A

Analytical solution 1D melting problem

```
1
2 %% Analytical solution for water-ice system
3
4 T1 = 323; %temperature liquid [K]
5 T2 = 253; %temperature solid [K]
6 Tm = 273.15; %melting temperature
7 L = 333*1000; %latent heat
8
9 %Properties fluid
10 lambda_f = 0.6435;
11 rho_f = 988.03;
12 cp_f = 4180.6;
13 alpha_f = lambda_f/(rho_f*cp_f);
14
15 %Properties solid
16 lambda_s = 2.4;
17 rho_s = 920.3;
18 cp_s = 1960;
19 alpha_s = lambda_s/(rho_s*cp_s);
20
21 %Solving for p
22 A = lambda_f * ((Tm-T1)/(sqrt(pi*alpha_f)));
23 B = L*rho_s*sqrt(alpha_f);
24 C = lambda_s*((T2-Tm)/sqrt(pi*alpha_s));
25
26 x1 = @(p) A*(exp(-p^2)/erf(p));
27 x2 = @(p) B*p;
28 x3 = @(p) C*(exp(-p^2*(alpha_f/alpha_s))/erfc(p*sqrt(alpha_f/alpha_s)));
29
30 f1 = @(p) (x1(p) + x2(p) - x3(p));
31 x0 = [0.001 50] ; %initial interval
32 options = optimset ('Display','Iter') ; % show iterations
33 [p,fval,exitflag,output] = fzero (f1 ,x0 ,options) ;
34
35 %Make data for plot
36 for i=1:85;
37     length_melted (i) = i*0.0001;
38     t_melt (i)= (0.5*length_melted(i)/p)^2 /alpha_f;
39 end
```

B

K-factor and drainage time

```
%% Determination K-factor for opening of 5 cm
clear all; close all; clc;

%data from COMSOL
P1 = importdata('Kfactortabel.txt');
kfactordata = P1.data;

v_av = 0.5*(kfactordata(:,2)+kfactordata(:,3)); %average velocity
deltaP = kfactordata(:,4)-kfactordata(:,5); %pressure difference

%General properties system and properties molten salt
rho = 4130;
g = 9.81;
h_plug = 0.4; %length pipe over freeze plug
y = 2*(deltaP./rho);
v2 = v_av.^2;

%Linear fit
p = polyfit(v2,y,1);
y1 = p(1)*v_av.^2+p(2);
Kfactor = p(1);

figure()
hold on
plot(v_av,y);
plot(v_av,y1,'r');
xlabel 'v (m/s)'; ylabel '2\Deltap /rho'; title 'Determination K-factor';
legend('Solutions from COMSOL model','Polynomial fit','Location','Northwest');
hold off

%% Development height of liquid in reactor vessel

H = 2.84; %height reactor vessel
Rtank = 1.42; %radius reactor vessel
Rpipe = 0.1; %radius drainage pipe
f = 0.0034; %Fanning friction factor

sumK = 0.5 + Kfactor;
L = 4/3; %total length pipe
l = L - h_plug; %length for wall friction

t = 0:0.01:300;
term = sqrt(2*g/(1+4*f*(l/(2*Rpipe))+sumK))*(Rpipe/Rtank)^2;
```

```
44 h_tank = 0.25*term^2*t.^2-sqrt(H+L)*term*t+H;
45
46 figure()
47 plot(t,h_tank);
48 xlabel 'time (s)'; ylabel 'Height liquid in vessel (m)'; title 'Drainage time
       narrow opening';
49 axis([0 300 0 3]);
```